STRUCTURE-ACTIVITY RELATIONSHIPS

IN

WERNER CLATHRATES

A thesis submitted to the

UNIVERSITY OF CAPE TOWN

in fulfilment of the requirements for the degree of

DOCTOR OF PHILOSOPHY

by

MADELEINE HENRIETTA MOORE

B.Sc.(Hons) (Natal, Pietermaritzburg)

Department of Physical Chemistry

University of Cape Town

Rondebosch

7700

Republic of South Africa

February 1987

ACKNOWLEDGEMENTS

Acknowledgement is due to:

My supervisor, Professor L. R. Nassimbeni, for his enthusiastic and patient guidance.

Dr M. L. Niven for her constant generosity with both her time and expertise.

All colleagues for their help and interest, especially to Michael Taylor and Dianne Bond.

Neil Ravenscroft, for his support and encouragement.

The University of Cape Town and A.E.C.I. for the financial assistance.

This work is dedicated to my father.

PUBLICATIONS

Parts of this work have been published.

1. Studies in Werner Clathrates. Part 2. Structures of bis(isothiocyanato)tetra(4-phenylpyridine)nickel(II).4dimethylsulphoxide, bis(isothiocyanato)tetra(3-methylpyridine)nickel(II).chloroform and bis(isothiocyanato)tetra(3,5-dimethylpyridine)nickel(II). L. R. Nassimbeni, S. Papanicolaou, M. H. Moore; **Journal of Inclusion Phenomena, 4,** 31 (1986).

2. Studies in Werner Clathrates. Part 3. Structures of bis(isothiocyanato)tetra(4-vinylpyridine)nickel(II) and its clathrates with ortho-, meta- and para-xylenes. M. H. Moore, L. R. Nassimbeni, M. L. Niven, M. W. Taylor; **Inorganica Chimica Acta, 115,** 211 (1986).

3 Studies in Werner Clathrates. Part 4. Structures of bis(isothiocyanato)tetra(4-ethylpyridine)nickel(II) and its clathrates with para-, meta-, and ortho-xylenes, carbon disulphide and carbon tetrachloride. M. H. Moore, L. R. Nassimbeni, M. L. Niven; **J. Chem. Soc. Dalton Transactions,** in publication.

4 Studies in Werner Clathrates. Part 5. Thermal analysis of bis(isothiocyanato)tetra(4-vinylpyridine)nickel(II) inclusion compounds. Crystal structure of the $[Ni(NCS)_2(4\text{-}Vipy)_4].2CHCl_3$ clathrate.

M. H. Moore, L. R. Nassimbeni, M. L. Niven; **Inorganica Chimica Acta**, in publication.

5 Studies in Werner Clathrates. Part 6. Structures of two novel polymeric inclusion compounds: poly(bis(isothiocyanato)di(2-aminopyridine)nickel(II). diethyl ether and di(aqua bis(isothiocyanato)3-aminopyridine μ-3-aminopyridine nickel(II)).water.
M. H. Moore, L. R. Nassimbeni, M. L. Niven; **Inorganica Chimica Acta**, in publication.

ABSTRACT

This work reports the synthesis and characterization of a series of inorganic coordination compounds which, upon crystallization, have the ability to include solvent or guest molecules spatially within the lattice. The compounds have the general formula:

a) $[NiX_2B_4]$: where X is isothiocyanate or bromine and B is 4-ethylpyridine, 4-vinylpyridine or 3,5-dimethylpyridine.

b) $[NiX_2B_2]_n$: where X is isothiocyanate, B is 2-aminopyridine and n indicates it is polymer.

c) $[NiX_2AB_2]_2$: where X is isothiocyanate, B is 3-aminopyridine (two of these four ligands in the dimer are bridging) and A is water.

The various guest molecules have been carefully chosen, according to their point symmetry, which is a key factor in yielding structures of a particular type.

The structures of seventeen compounds have been elucidated by single crystal X-ray analysis. The difficulty has been found to lie in refining disordered guest molecules. Other techniques employed in the initial characterization of these compounds are Microanalysis, Mass Spectrometry and UV/Visible Spectrophotometry.

An intramolecular potential energy study on the $[Ni(NCS)_2(3,5\text{-diMepy})_4]$ complex reveals that the ortho-hydrogens on the 3,5-dimethylpyridine ligands control the conformation of the molecule.

Packing densities and volume comparisons of the $[Ni(NCS)_2(4\text{-Etpy})_4]$ and $[Ni(NCS)_2(4\text{-Vipy})_4]$ complexes and their clathrates have been carried out.

The exact sizes and shapes of the cavities in which the guest molecules are located in the X-ray crystal structures have been evaluated by both intermolecular potential energy and molecular volume calculations.

Thermodynamic and spectroscopic properties of the $[Ni(NCS)_2(4\text{-}Etpy)_4]$ and $[Ni(NCS)_2(4\text{-}Vipy)_4]$ clathrates have been studied in both solution and the solid state. The techniques used are X-ray powder diffractometry, IR spectroscopy and Thermogravimetry (including Differential Thermal Analysis).

CONTENTS PAGE

All Appendices are on microfilm:

APPENDIX A Bond lengths, angles and torsion angles in the structures of compounds I to XVII (1 microfilm)

APPENDIX B Analysis of variance tables for all the structures of compounds I to XVII (1 microfilm)

APPENDIX C Observed and calculated structure factors of structures I to XVII (8 microfilms)

CHAPTER 1

1 INTRODUCTION

1.1 Inclusion Compounds:

Inclusion compounds are formed when a particular type of molecule is able to include another, usually smaller, molecule spatially within its structure, leaving the bonding systems of both components unaffected. The terms `host' and `guest' are applied to the enclosing molecular network and the enclosed molecule respectively. An essential characteristic of the host molecule is, therefore, its ability to form a structure with hollow spaces of large enough dimensions to house prospective guests. Some typical shapes these guest-voids may adopt are illustrated in fig. 1.1. The stability of an inclusion compound is largely attributable to the way in which the molecules involved fit together in space.

'Inclusion chemistry', to quote Powell, 'has developed in its own right since the two words came into conjoint use through a confluence of two streams of thought'[1.1]. The first derives from the simple old observation that some natural objects, by virtue of their shape and construction, may act as containers of other things and the second is the theory of chemistry.

The history of the preparation of inclusion compounds can be traced back to the early 1800s when Wohler[1.2] and Clemm[1.3] made the first quinol clathrates; however at that stage structural chemistry was insufficiently developed for this kind of explanation. It was only in 1948, with the

Fig. 1.1

Some possible arrangements of host lattices

(Sci. Amer., July 1962).

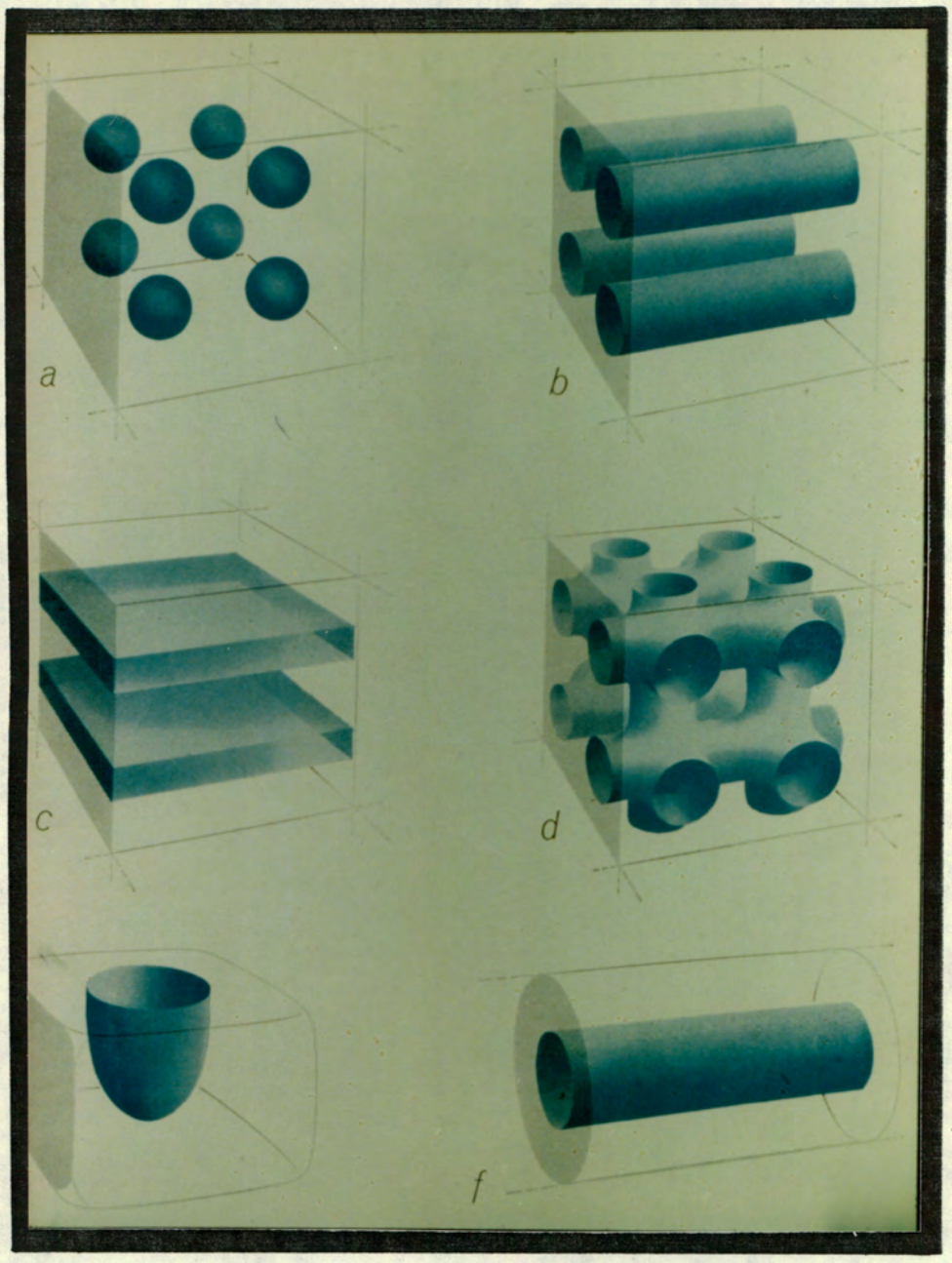

publication of H. M. Powell's papers on the structures and compositions of β-quinol clathrates[1.4], that the structure of an inclusion compound was first elucidated by accurate X-ray studies. This revealed complete enclosure of guest molecules by infinite three-dimensional complexes formed by hydrogen bonding between individual hydroquinone molecules and led to the coining of a new word `clathrate' to name this thorough type of inclusion compound. The word arose from an ancient word, 'clathratus', meaning closed or protected by the cross-bars of a trellis, which was explained in a dictionary concerning the social life and industrial arts of the Greeks and Romans; the entry is illustrated in fig. 1.2.

The variety of inclusion compound types is vast since it depends not only on the physico-chemical properties of the host and guest components but also on their numerical ratio and type of interaction between them.

The major forces operating in the formation of an inclusion compound depend on the type of compound being formed. Weak dispersion or Van der Waals forces are considered very important and highly oriented dipole interactions may be contributing factors. The wide applications associated with 'extramolecular chemistry' have encouraged a growing interest in the chemistry of 'weak interactions'[1.5].

The application of spatial 'fitting together' of molecules has already proved to be amazingly effective in the separation of molecules with similar physico-chemical properties. The synthesis of host lattices with 'tailor-made' specificity for various isomers, enantiomers or even

Fig.1.2 Entries in 'A dictionary of Roman and Greek Antiquities' (A. Rich; Longmans Green, London, Revised 1884).

CLATHRA'TUS. Closed or protected by cross-bars of trellis (*clathri*), as explained in the next paragraph. Plaut. *Mil.* ii. 4. 25.

CLA'THRI. A *trellis* or grating of wood or metal employed to cover over and protect an aperture, such as

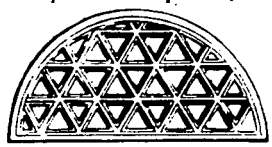

a door or window, or to enclose anything generally. (Hor. *A. P.* 473. Plin. *H. N.* viii. 7. Cato, *R. R.* iv. 1. Columell. viii. 17. 10.) The example represents the trellis which covered in the lunettes over the stalls (*carceres*) in the circus of Caracalla.

Fig.1.3 Polymerization of 2,3-dimethylbutadiene in the thiourea channel[1.10].

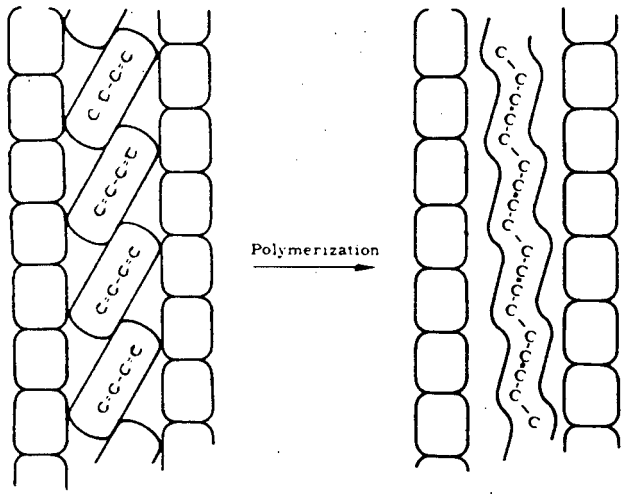

isotopomers is practically possible, for example with host molecules of either tri-o-thymotide[1.6] or Hoffmann-type complexes[1.7].

Study into the way in which the reactivity of a molecule, a guest, is governed by its environment, the host, has increased as inclusion compounds are more extensively used as enzyme models[1.8]. An early study in this area concerned the preferential formation of stereo-regular polymers from unsaturated molecules entrapped in the channels of urea[1.9] and thiourea[1.10], as shown in fig.1.3. Since then inclusion polymerisation has been carried out in a number of host lattices[1.11].

A relatively new application of inclusion compounds is their use as highly selective chemical reagents. An example, which is illustrated in fig. 1.4, concerns the use of bromine included in Zeolite 5A as a selective brominating agent of styrene in mixtures of the latter with cyclohexene[1.12]. The included bromine is only accessible to the styrene double bond since its aliphatic chain can penetrate the cavity, an impossible task for cyclohexene's double bond to perform.

Inclusion compounds have also found application as sources and reservoirs of unstable species. The cyclodextrins[1.13] provide the sure example of enclosure by a single molecule with a suitable hole in the middle (an intramolecular host-guest aggregate). The fact that they may be regarded as natural products and that their imprisoning action takes place also when they are in solution has led to their development as efficient delivery systems for anti-cancer drugs.

Fig 1.4

The bromination reactions of styrene and cyclohexene[1.12].

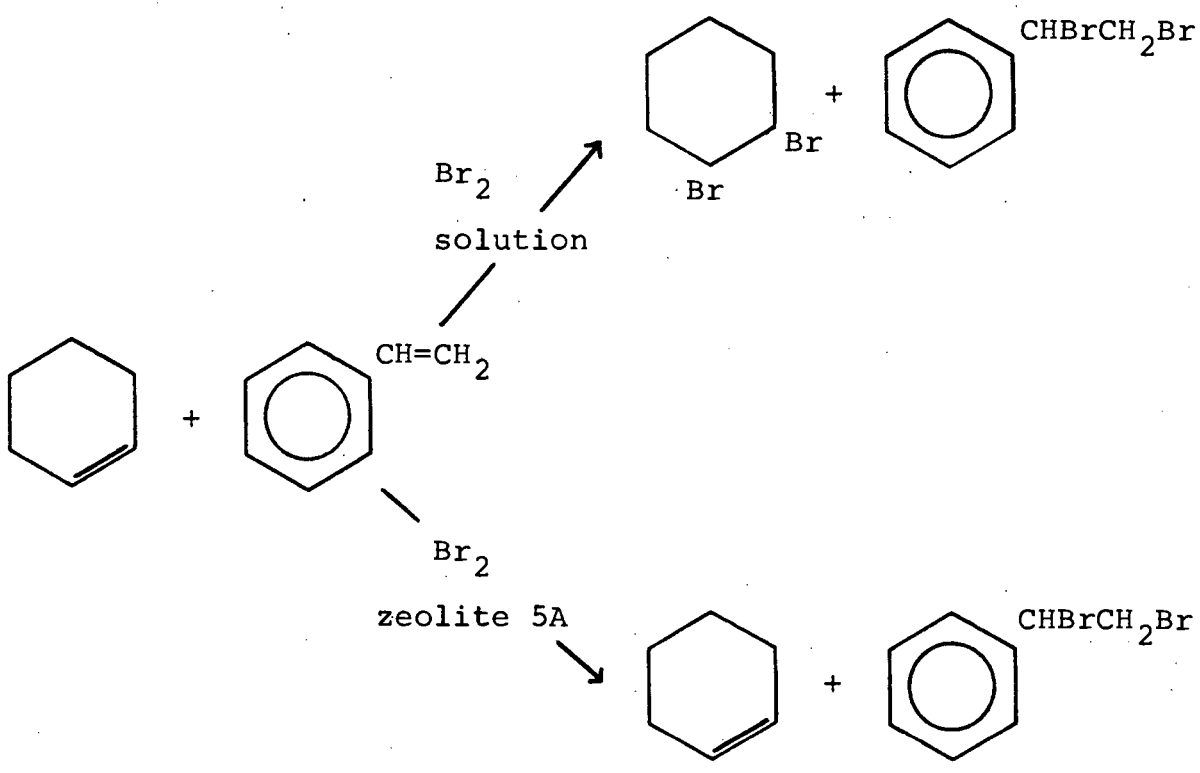

X-ray diffraction studies on proteins, synthetic fibres, cellulose, rubber, crystalline viruses, vitamins and others have revealed the inclusion properties of many of these naturally occurring compounds. Intramolecular folding in polypeptide chains, α-helix structures as in α-keratin, and the various forms of hemoglobin in whose wet crystals alternate layers of protein and liquid of crystallization are found, all indicate the eventual delineation of inclusion characteristics.

The recent exponential growth in host-guest chemistry has resulted in a vast increase in the number and variation of new host molecular structures which have necessitated a definite classification of these host molecular structures[1.14]. This is based on the criteria of:

a) Host-guest type and the type of interaction between the two components.
b) The topology of the host-guest aggregate.
c) The number of the various components forming the aggregate.

In this characterization Powell's original definition of a clathrate, which necessitated complete enclosure of the guest, was broadened to state merely that the guest is retained by steric barriers.

1.2 Werner Clathrates:

A Werner clathrate (named after the pioneer of coordination chemistry, Alfred Werner) is an inclusion complex with a host framework made up of transition metal coordination complexes represented by the general formula $[MX_2B_4]$ where, M is a divalent transition metal cation (eg: Fe^{2+}, Co^{2+}, Ni^{2+}, Cu^{2+}, Zn^{2+}, Cd^{2+}), X denotes the anionic ligand (eg: NCS^-, NCO^-, CN^-, NO_3^-, NO_2^-, Br^-, Cl^-, I^-) and B represents an electrically neutral substituted pyridine, α - arylalkylamine or isoquinoline. The variation of these complexes is vast since the possibility of isomerism and/or complexation by more than one type of B ligand exists.

These Werner complexes form extramolecular host-guest aggregates in which the guest is retained by steric barriers formed by the host lattice (crystal lattice forces).

Interest in Werner clathrates was stimulated by Schaeffer and coworkers who announced their use in the separation of various aromatic hydrocarbons from petroleum fractions[1.15]. [1.20]

The most thoroughly studied complex thus far investigated has been $[Ni(NCS)_2(4\text{-Mepy})_4]$ which can entrap a wide variety of guest molecules ranging from noble gases to condensed aromatic hydrocarbons, in cavities of the channel, layer or cage type. The formation of these inclusion compounds is stereoselective and may be used for the separation of isomer mixtures[1.16] and even isotopomers[1.17]. The structures and thermodynamics of the clathration process with this complex forming the host framework have recently been reviewed by Lipkowski[1.18, 1.19].

Host complexes of this type are synthesised by the double decomposition of nickel chloride with thiocyanate salt, and subsequent addition of the aromatic ligand. Crystallization of the host in the presence of the guest is sufficient to obtain the clathrate.

X-ray crystallography has revealed that the MX_2B_4 molecules usually have irregular octahedral coordination and are 'overcrowded' in their central region ie: there are non-bonded repulsive interactions between the ligands which lead to a limited number of stable conformations. The most common one is a 'propeller' conformation: in the $[Ni(NCS)_2(4\text{-}Mepy)_4]$ molecule, for example, the four pyridine rings are twisted by 43° - 55° from the coplanar arrangement. It is believed that an essential feature affecting the clathrating ability of the $[Ni(NCS)_2(4\text{-}Mepy)_4]$ molecule is the conformational freedom of its pyridine rings which is achieved by their ability to rotate, to a certain degree, about their corresponding Ni - N bonds. In this manner the complex is able to 'adjust' its molecular shape and make possible clathration of guest molecules differing in size, shape and polarity.

Most of the inclusion forming $[MX_2B_4]$ complexes contain thiocyanate groups as the anionic ligands (X^-). Usually these groups are bound to the central metal atom through the nitrogen atom (isothiocyanates) in such a way that they are trans to each other and each one is bent at its nitrogen atom. The M - N_{cs} - C_s bond angle ranges from 154° - 175° and is governed in part by both intra- and intermolecular interactions.

Substitution on the pyridine ring (B) results in a decrease in the packing efficiency of the $[MX_2B_4]$ molecules which makes spaces available for guest occupation in the crystalline state.

1.2.1 The $[Ni(NCS)_2(4\text{-Mepy})_4]$ Werner complex:

Depending on the solvent type, the $[Ni(NCS)_2(4\text{-Mepy})_4]$ complex may crystallise in either a compact non-clathrating lattice type, designated the α-phase by Hart and Smith[1.20], or in a porous clathrating phase, designated the β-phase by the same authors. They reported the maximum possible aromatic guest content in the β-phase to exist when the guest : host ratio is 1 : 1. Subsequently Lipkowski et al[1.21] found that if the concentration of aromatic guest is sufficient (> 0.5M) a clathrate with a different crystalline phase , designated the γ-phase, is formed. The γ-phase clathrates were found to be firstly less stable than original β-phases and secondly to have a maximum guest : host ratio of 2 : 1.

Subsequent X-ray crystallographic studies on these phases have revealed similar overall $[Ni(NCS)_2(4\text{-Mepy})_4]$ molecular configurations in all phases[1.22-1.24]; thus practically all differences between them are concerned with the packing of these molecules which is in turn dependent on the solvent from which they crystallise.

All the β-phase clathrates of $[Ni(NCS)_2(4\text{-Mepy})_4]$ crystallise in the tetragonal space group $I4_1/a$ in such a way that the host molecules leave a three-dimensional system of cavities interlinked by channels of guest molecular

size[1.25]. This type of structure contains two different cavities, or 'adsorption centres', of $\bar{1}$ and $\bar{4}$ local symmetry available for guest molecules. Until now only occupation of the $\bar{1}$ cavities has been revealed in single-crystal studies. The latter have shown how a single aromatic guest molecule fills the $\bar{1}$ site and how two smaller molecules (eg: methanol) are required to fill the same site[1.23].

Although the crystal symmetry may differ from one guest to another, the overall structure of a γ-phase $[Ni(NCS)_2(4\text{-}Mepy)_4]$ clathrate is composed of layers formed by the host molecules. Guest molecules are located in cavities confined by the isothiocyanate groups which protrude into the space between host layers. These layered structures are stable only in the presence of guest molecules while the zeolite-like β-phase preserves its porosity even in the absence of guest molecules, a feature that has been exploited to obtain thermodynamic information in this type of lattice[1.26]. Both clathrating phases can alter their porosity in order to absorb bigger or smaller guest molecules.

Kinetic studies[1.26] on the course of the reaction:

$$\alpha\text{-}[Ni(NCS)_2(4\text{-}Mepy)_4] + G_{liq} \longrightarrow \beta\text{-}[Ni(NCS)_2(4\text{-}Mepy)_4].G$$

together with sorption equilibria in solid clathrate compound - liquid guest solution systems[1.20] and absorption studies of guest from the gas phase[1.27] have revealed that the clathration process does not involve a dissolution-crystallization process. Alternatively, when the concentration of a suitable guest reaches a threshold value, $\alpha \longrightarrow \beta$ -phase reconstruction in the solid phase takes place.

Practically important for separation purposes are equilibria in systems where competitive absorption of different guests takes place at different sites in the host lattice[1.26, 1.28]. These reflect the strong influence a guest's molecular structure has on the number and shape of the cavities in the host framework.

Macroscopically, energy of guest-lattice interactions, which reflects the overall stability of the clathrate, appears as the enthalpy of the enclathration reaction, (ΔH_{clath}):

α-[Ni(NCS)$_2$(4-Mepy)$_4$] + nG $\longrightarrow$ β-[Ni(NCS)$_2$(4-Mepy)$_4$].nG

Thermochemical studies on this enclathration reaction were initiated by Hart and Smith[1.20] who subdivided the total enthalpy, ΔH_{clath}, into the components:

$$\Delta H_{clath} = \Delta H_{\alpha \rightarrow \beta} + \Delta H_{evap} + \Delta H_{sorp}$$

such that:

a) $\Delta H_{\alpha \rightarrow \beta}$ = enthalpy associated with lattice transformation from the α- to β-phase.

b) ΔH_{evap} = enthalpy of conversion of the guest compound into the gaseous state.

c) ΔH_{sorp} = enthalpy of sorption of gaseous guest molecules by the clathrating β-structure.

However, it has subsequently been found that the $\Delta H_{\alpha \rightarrow \beta}$ component cannot be assumed to be constant (ie: independent of the type of guest component) because of the dilation-contraction which occurs when either sorption-desorption of the guest or its exchange with another type of guest takes place in the β-clathrate. It has therefore been split into two components:

i) $\Delta H_{\alpha \rightarrow \beta_0}$ corresponding to the $\alpha \rightarrow \beta_0$ phase transition, where β_0 denotes `empty' β-structure, which is

independent of guest type. This value has been determined experimentally[1.29].

ii) $\Delta H_{\beta_0 \rightarrow \beta}$ which denotes the enthalpy of β-structure dilation occurring on absorption of the guest and may be derived for each guest type[1.18].

This indicates a possible mechanism for clathration being initially a fast $\alpha \rightarrow \beta_0$ transformation in the solid lattice followed by a slow lattice change from β_0 to β with absorption of guest molecules.

The rate of desorption of a guest from a β-$[Ni(NCS)_2(4\text{-Mepy})_4]$ lattice is limited either by diffusion through the channel structure or by breaking the guest-host bindings. Ortho- and meta-substituted dinitrobenzenes have the slowest diffusion rates owing to their molecular shape which does not permit easy diffusion through the narrowings in the β-structure. The more streamlined centrosymmetric para isomer, however, does not diffuse much faster through this lattice type because it is the best fitting guest to its 'para' selective cavities. So in this case the breaking of guest-host 'bonds', rather than diffusion, is the rate determining step[1.26].

1.2.2 Clathrating ability and selectivity

It is commonly agreed that the clathrating ability of these Werner complexes depends on their molecular structure and in particular on the pyridine ligand. An investigation into the structural and stability changes which occur with variations in the pyridine ligand is the primary aim of the present

study. One variation in the anionic ligand has also been examined.

The selectivity of enclathration is thought to depend on the shape more than the volume of the potential guest molecule, and on the shape of the neutral ligands.

Specific chemical host - guest interactions such as charge-transfer processes have been eliminated as factors contributing to the sorption properties since good overlap of the pyridine rings and aromatic parts of guest molecules is geometrically impossible; thus selective enclathration seems to be almost entirely based on steric considerations.

The strong guest influence on the clathrating host lattice type in $[Ni(NCS)_2(4\text{-Mepy})_4]$ clathrates is illustrated by the fact that across almost the whole range of possible compositions of the ortho, meta and para xylene isomers the thermodynamically stable host lattice is the β-phase which is 'para' selective. However, at high o-xylene and low p-xylene concentrations the stable crystal lattice is the layer-type γ-phase which is 'ortho' selective[1.24].

No correlation between selectivity and enthalpy of inclusion has been observed for this Werner complex, which highlights the importance of dynamic factors in determining the selectivity of inclusion.

Host lattices of the type $[Ni(NCS)_2(R^2\text{-}C_6H_4\text{-}(CH\text{-}R^1)\text{-}NH_2)_4]$ where R^1 = Me, Et, Pr... etc, and R^2 = H, p-Me, o-Me... etc have also shown selectivity among various xylenes and methyl-naphthalenes[1.30]. The greater flexibility of these neutral ligands about their metal coordinating nitrogen and the subsequent location of their aromatic rings allow for

some weak electronic host : guest interactions. The presence of chiral ligands introduces the possibility of enantiomeric selectivity[1.31].

1.2.3 $[NiX_2B_2]$ Werner complexes:

Inclusion compound formation from two-base complexes of the type $[Ni(NCS)_2B_2]$ has not been as extensively studied.
This work was stimulated by a previous study[1.32] on the dependence of the stereochemistry of $[Ni(NCS)_2(q\text{-}Rpy)_2]$ complexes on various positions of a substituent (q = 2,3 or 4) on the pyridine ligand (py), as well as on the nature of the substituent (R = Me, Et, NH_2, Cl, Br and CN). The authors reported association of solvent molecules when 2-NH_2py was used as the neutral ligand.
Molecular structures have largely been determined by magnetic and spectral measurements[1.30, 1.32]; however X-ray structure analyses have been carried out on $[Ni(NCS)_2(2,5\text{-}diMepy)_2]$[1.33], $[Ni(NCS)_2(piperidine)_2].C_6H_6$[1.34] and $[Ni(NCS)_2(3\text{-methyl isoquinoline})_2]$[1.35].
In mononuclear $[Ni(NCS)_2(2\text{-}Rpy)_2]$ structures the substituent in the 2-position shows steric interaction with the thiocyanate groups resulting in destabilization of the structure. However stabilization can be achieved by the lengthening of the Ni-N(py) bond and by the twisting of the pyridine ring from the equatorial plane, as supported by X-ray structure analysis results for the $[Ni(NCS)_2(2,5\text{-di Mepy})_2]$ complex[1.33]. The 2-substituent of the twisted pyridine ring in this case makes the interaction in axial positions more difficult, contrary to the effect of

substituents in positions 3 or 4.

1.2.4 Industrial uses:

Although the selectivities among ortho, meta, and para isomers shown by $[Ni(NCS)_2(4\text{-Mepy})_4]$ and $[Ni(NCS)_2(\alpha\text{-arylalkylamine})_4]$ host lattices have been put to good use in small scale separations and in chromatographic applications[1.36], a disappointing aspect of their industrial applications is the absence of any large scale commercial separation plants. The Union Oil Company built a pilot plant to separate meta and para xylene using the selectivity of $[Ni(NCS)_2(4\text{-Mepy})_4]$ for the para isomer, and fig. 1.5 illustrates the flow diagram for the Labofina process for separating meta and para xylene using the selectivity of $[Ni(NCS)_2(\alpha\text{-(m-chlorophenyl)ethylamine})_4]$ for the para isomer[1.37].

The main problem in commercial scale separation plants would be the need to handle solids with the concomitant need for precipitation, filtration, and washing sequences which would require high cost filtration or centrifuge equipment and large volumes of washing liquid.

These difficulties may possibly be overcome by the use of 'liquid clathrates', which are formed between host compounds of the general formula $[M(Al_2(CH_3)_6X)]$, where M = alkali metal or tetraalkylammonium ion; X = N_3, SCN, SeCN, F, Cl, Br, I, and small aromatic guest molecules[1.38].

Fig.1.5 Flow diagram for the Labofina process for separating meta and para xylenes[1.37].

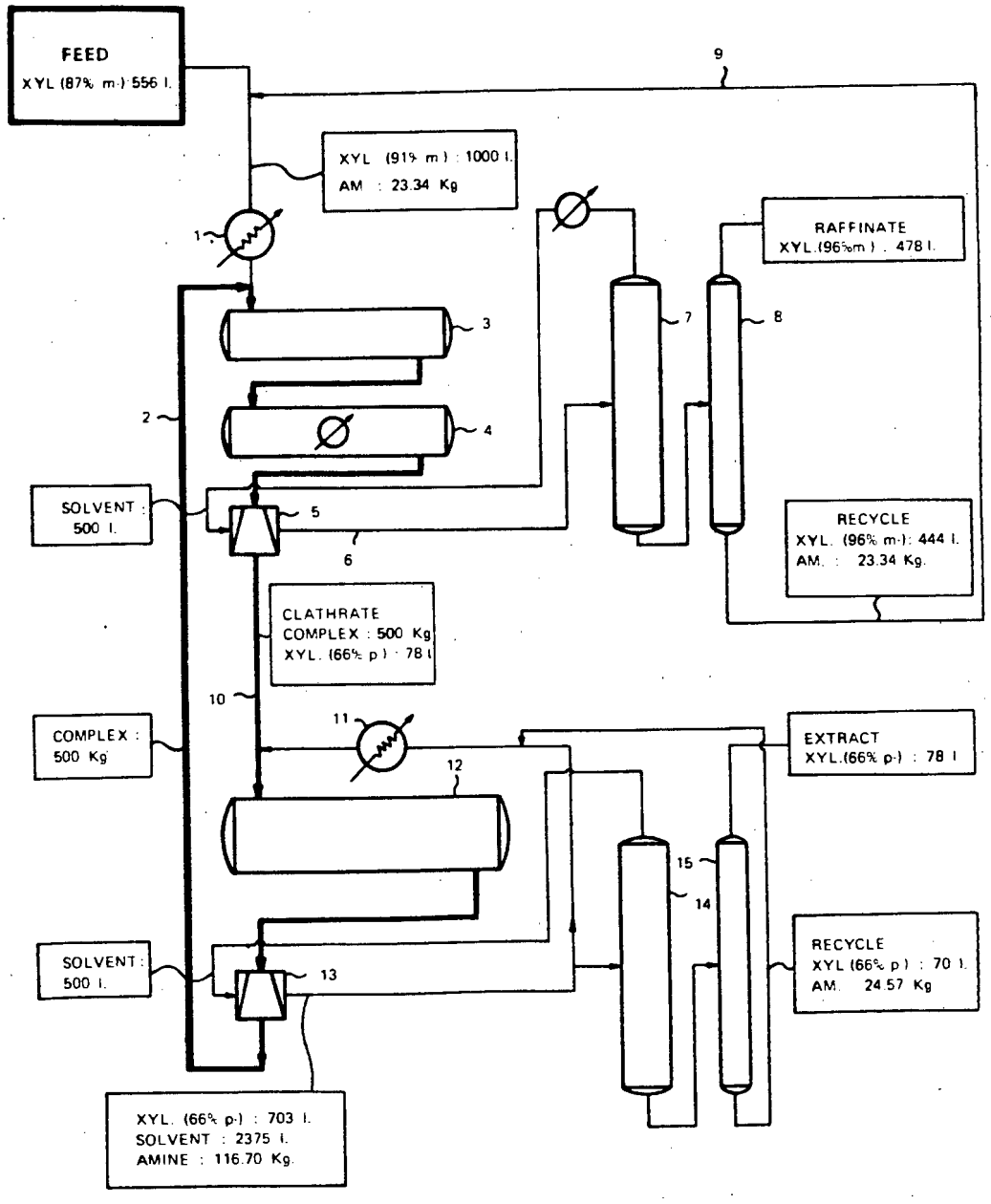

The importance of this field of chemistry is reflected in the increasing number of publications dealing with host-guest interactions. In particular, a new journal, entitled ' Journal of Inclusion Phenomena ', emerged in 1983 with the express purpose of reporting original research ' into all aspects of the study of host-guest systems '.

1 REFERENCES

1.1 H. M. Powell; `Inclusion Compounds'; edited by J. L. Atwood, J. E. D. Davies, D. D. MacNicol; Academic Press, New York, vol 1, chapter 1 (1984).

1.2 F. Wohler; **Justus Liebigs Ann. Chem., 69,** 297 (1849).

1.3 A. Clemm; **Justus Liebigs Ann. Chem., 110,** 357 (1859).

1.4a) H. M. Powell; **J. Chem. Soc.,** 61 (1948).

b) D. E. Palin, H. M. Powell; **J. Chem. Soc.,** 815 (1948).

1.5 R. M. Kellogg; **Top. Curr. Chem., 101,** 11 (1982).

1.6 R. Arad-Yellin, B. S. Green, M. Knossow, G. Tsoucaris; **J. Am. Chem. Soc., 105,** 4561 (1983).

1.7 T. Iwamoto;`Inclusion Compounds'; edited by J. L. Atwood, J. E. D. Davies, D. D. MacNicol; Academic Press, New York, vol 1, chapter 2 (1984).

1.8 R. Breslow; **Science, 218,** 532 (1982).

1.9 D. W. White; J. **Am. Chem. Soc., 82,** 5678 (1960).

1.10 J. F. Brown, D. W. White; **J. Am. Chem. Soc., 82,** 5671 (1960).

1.11 M. Farina; **Makromol. Chem., Suppl., 4,** 21 (1981).

1.12 P. A. Risbood, D. M. Ruthven; **J. Am. Chem. Soc., 100,** 4919 (1978).

1.13 W. Saenger; `Inclusion Compounds'; edited by J. L. Atwood, J. E. D. Davies, D. D. MacNicol; Academic Press, New York, vol 2, chapter 8 (1984).

1.14 E. Webber, H. P. Josel; **J. Incl. Phenom., 1,** 79 (1983).

1.15 W. D. Schaeffer, W. S. Dorsey, D. A. Skinner, J. Christian; **J. Am. Chem. Soc., 79,** 5870 (1957).

1.16 P. Starzewski, J. Lipkowski; **Pol. J. Chem., 53,** 1869 (1979).

1.17 S. E. Ofodile, R. M. Kellett, N. O. Smith; **J. Am. Chem. Soc., 101,** 7725 (1979).

1.18 J. Lipkowski; `Inclusion Compounds'; edited by J. L. Atwood, J. E. D. Davies, D. D. MacNicol; Academic Press, New York, vol 1, chapter 3 (1984).

1.19 J. Lipkowski, P. Starzewski, W. Zielenkiewicz; **Pol. J. Chem., 56,** 349 (1982).

1.20 M. I. Hart, N. O. Smith; **J. Am. Chem. Soc., 84,** 1816 (1962).

1.21 W. Kemula, J. Lipkowski, D. Sybilska; **Roczniki Chemii, 48,** 3 (1974).

1.22 I. S. Kerr, D. J. Williams; **Acta Cryst., B33,** 3589 (1977).

1.23 J. Lipkowski, K. Suwinska, G. D. Andreetti, K. Stadnicka; **J. Mol. Struct., 75,** 101 (1981).

1.24 J. Lipkowski, G. D. Andreetti; **Acta Cryst., B38,** 607 (1982).

1.25 E. R. de Gil, I. S. Kerr; **J. Appl. Crystallogr., 10,** 315 (1977).

1.26 J. Lipkowski, P. Starzewski, W. Zielenkiewicz; **Thermochim. Acta, 49,** 269 (1981).

1.27 S. A. Allison, R. M. Barrer; **J. Chem. Soc., A,** 1717 (1969).

1.28 M. J. Minton, N. O. Smith; **J. Phys. Chem., 71,** 3618 (1967).

1.29 J. Lipkowski, J. Chajin; **Roczniki Chemii, 51,** 1443 (1977).

1.30 J. Hanotier, P. de Radzitzky; `Inclusion Compounds'; edited by J. L. Atwood, J. E. D. Davies, D. D. MacNicol; Academic Press, New York, vol 1, chapter 4 (1984).

1.31 L. R. Nassimbeni, M. L. Niven, K. J. Zemke; **Acta Cryst., B42,** 453 (1986).

1.32 M. Jamnicky, E. Jona; **Inorg. Chim. Acta, 88,** 1 (1984).

1.33 E. Durcanska, T. Glowiak, J. Kozisek; **Chem. Zvesti, 36 (5),** 651 (1982).

1.34 M. Koman, E. Durcanska, M. Handlovic, J. Gazo; **Acta Cryst., C41,** 1418 (1985).

1.35 M. Goodgame, M. J. Weeks; **J. Chem. Soc., A,** 1156 (1966).

1.36 D. Sybilska, E. Smolkova-Keulemansova; `Inclusion Compounds'; edited by J. L. Atwood, J. E. D. Davies, D. D. MacNicol; Academic Press, New York, vol 3, chapter 6 (1984).

1.37 J. Hanotier; **Ind. Chim. Belg., 31,** 19 (1966).

1.38 J. L. Atwood; `Inclusion Compounds'; edited by J. L. Atwood, J. E. D. Davies, D. D. MacNicol; Academic Press, New York, vol 1, chapter 9 (1984).

CHAPTER 2

2 EXPERIMENTAL

All compounds studied together with the numbers and codes which refer to them are listed in table 2.1.

2.1 Preparation of $[NiX_2B_4]$ Complexes and their clathrates, where X = NCS^- or Br^- and B = 4-Etpy, 4-Vipy or 3,5-diMepy .

All reagents and solvents used were analytically pure and generally supplied by SARchem (Johannesburg); only the substituted pyridines were obtained from the Aldrich Chemical Company (Germany). All preparations were carried out with glass distilled water and crystallizations were done at room temperature (294-303K). Decomposition temperatures were determined on a Reichert Thermovar melting point apparatus.

2.1.1 Preparation of $[Ni(NCS)_2(4\text{-Etpy})_4]$, $[Ni(NCS)_2(4\text{-Vipy})_4]$ and $[Ni(NCS)_2(3,5\text{-diMepy})_4]$ host powder complexes:

Host powder complexes were prepared by the method of Schaeffer et al[2.1] as follows:

A green transparent solution of $Ni(NCS)_2$ (8.4mmole) was made by dissolving nickel chloride, $NiCl_2.6H_2O$, (2.00g, 8.4mmole) and potassium thiocyanate, KSCN, (1.64g, 16.8mmole) in distilled water (20ml). The substituted pyridine (36.9mmol - a 10% excess) was added dropwise (over approximately 5 minutes) with constant stirring to the green solution. An immediate fine pale blue-purple

TABLE 2.1 The compounds studied together with the numbers and codes which refer to them.

Compound Formula*	Compound Number	Code Name
$[NiX_2(4\text{-Etpy})_4]$	I	NYET
$[NiX_2(4\text{-Etpy})_4]$	II	NICH
$[NiX_2(4\text{-Etpy})_4].1/2\ CCl_4$	III	NICL
.p-xylene	IV	NIPAX
.m-xylene	V	NIMEX
.o-xylene	VI	NIORX
.2 CS_2	VII	CSDE
.2 CCl_4	VIII	NIGL
$[NiX_2(4\text{-Vipy})_4]$	IX	NIVTH
.p-xylene	X	NIVP
.m-xylene	XI	NIVMEX
.o-xylene	XII	NIVOX
.2 $CHCl_3$	XIII	NIVBU
.1,8 THF**		
.Ø,25 4-Vipy**		
$[Ni(Br)_2(4\text{-Etpy})_4].2H_2O$	XIV	NIEBB
$[NiX_2(3,5\text{-diMepy})_4]$	XV	LIVY
$[NiX_2(2\text{-}NH_2py)_2]$.diethyl ether	XVI	TAPY
$[NiX_2(3\text{-}NH_2py)_2H_2O].H_2O$	XVII	TRIPY

* Where: X = NCS^-

4-Etpy = 4-ethylpyridine

4-Vipy = 4-vinylpyridine

THF = tetrahydrofuran

3,5-diMepy = 3,5-dimethylpyridine

2-NH_2py = 2-aminopyridine

3-NH_2py = 3-aminopyridine

** A compound not used for X-ray crystallographic studies was not given a name and code.

precipitate (the host powder complex) formed. The mixture was stirred for an additional 30 minutes after all the ligand had been added to ensure complete reaction, then the precipitate was filtered (Büchi Apparatus), washed with distilled water (3 x 10ml) and air dried for 30 minutes then finally placed in a desiccator for 24 hours.

An attempt was made to determine the melting point of each host powder. However when subjected to heat, the powders first went pale green at approximately 130^{o}C then started to go yellow at 135^{o}C and had eventually decomposed to a brown powder by 250^{o}C. The thermal decomposition was subsequently studied; in section 5.4 these results are discussed in detail.

2.1.2 Preliminary solubility studies and solvent choice.

Initially the solubilities of the host powders in various solvents were qualitatively determined; the observations made for some solvents are listed in table 2.2.
All three hosts show marked differences in solubilities in the different solvents. The quantitative differences in solubilities of the $[Ni(NCS)_2(4\text{-}Etpy)_4]$ and $[Ni(NCS)_2(4\text{-}Vipy)_4]$ complexes in various solvents were determined (see section 5.1 for details).
Solutions of the $[Ni(NCS)_2(4\text{-}Etpy)_4]$ and $[Ni(NCS)_2(4\text{-}Vipy)_4]$ host powders in the solvents listed in table 2.2 were often slightly turbid. The pale green colloidal suspension formed in each case was filtered off (it never amounted to more than 2% by weight of the orginal host powder dissolved) and

TABLE 2.2 **Preliminary qualitative solubility observations.**

Solvent	$[Ni(NCS)_2L_4]$ where L = 4-Etpy	4-Vipy	3,5-diMepy
THF, C_4H_8O	vS	vS	I
chloroform, $CHCl_3$	vS	vS	I
carbon tetrachloride, CCl_4	S	I	I
p-xylene, p-C_8H_{10}	S	pS	I
m-xylene, m-C_8H_{10}	S	S	I
o-xylene, o-C_8H_{10}	S	S	I
carbon disulphide, CS_2	S	S	I
dimethyl sulphoxide (DMSO), C_2H_6OS	vS	vS	S(h)
diethyl ether, $C_4H_{10}O$	I	I	I
bromoethane, C_2H_5Br	S	S	I

Where the solubility gradient is expressed as:

vS = Very soluble

S = Soluble

S(h) = Soluble only with heat

pS = Partially soluble

I = Insoluble

some attempt was made to characterise it (see sections 3.1.1, 3.1.2 and 5.2).

In order to prepare single crystals of the non-clathrated α-phase of each host powder a suitable solvent (ie: one which would not be enclathrated during crystallization of the Werner complex) had to be chosen.

Aromatics are highly suitable guest compounds, the Werner hosts are totally insoluble in long-chain aliphatic solvents and solvent molecules like CCl_4, $CHCl_3$ and CS_2 were found to be enclathrated so short-chain aliphatics and saturated cyclic solvents seemed the most promising.

From the likely solvents listed in table 2.2 both DMSO and bromoethane were eliminated because of their ability to substitute ligands on the Werner complex. X-ray diffraction studies on single crystals obtained from a DMSO solution of $[Ni(NCS)_2(4\text{-Phpy})_4]$[2.2] and a bromoethane solution of $[Ni(NCS)_2(4\text{-Etpy})_4]$ have revealed that DMSO can displace a pyridine ligand on the Werner complex by coordinating via its oxygen atom[2.2] and bromine can substitute the isothiocyanate groups (see compound XIV).

However DMSO was the only solvent that could be found for the $[Ni(NCS)_2(3,5\text{-diMepy})_4]$ host powder, and preliminary analyses on the crystals obtained indicated the presence of the Werner complex only.

The most suitable solvent found for crystal growth of the α-phases of the other two host complexes was THF.

2.1.3 Crystal growth of the host complexes.

The following solutions were used to crystallize the host complexes:

a) A saturated DMSO solution of $[Ni(NCS)_2(3,5diMepy)_4]$ obtained by heating the solvent to its boiling point.

b) A saturated THF (compound I) or chloroform (compound II) solution of $[Ni(NCS)_2(4\text{-}Etpy)_4]$ obtained with warming.

c) A half-saturated THF solution of $[Ni(NCS)_2(4\text{-}Vipy)_4]$.

Two basic methods of crystallization were employed:

a) Slow Evaporation:

The solutions were placed in tubes, covered with perforated plastic film and left to stand. The solvent evaporated and crystals formed on the edges of the tubes.

The DMSO solution evaporated slowly enough for good quality deep purple-blue octahedral crystals of $[Ni(NCS)_2(3,5\text{-}diMepy)_4]$ to grow. However both THF and chloroform evaporated too quickly for crystals of satisfactory quality for structural studies to grow and thus the liquid diffusion method was chosen instead.

b) Liquid Diffusion[2.3]:

The solutions were placed in tubes (10mm diameter); then a suitable precipitating solvent was layered carefully down the side of each tube onto the surface of the solution in the tube (an immediate turbidity occurred as the interface was being established). The precipitant chosen was diethyl

ether because it is less dense than and miscible with both THF and chloroform and the host complexes are insoluble in it. The tubes were stoppered immediately after layering was complete and left to stand undisturbed. As the THF or chloroform diffuses into the diethyl ether blue needle-shaped crystals of the host complex (compounds I, II and IX) form at the interface. Diffusion was maintained at a minimal rate by keeping the amount of disturbance and surface area to a minimum (hence the choice of tubes with a small diameter) to ensure good quality single crystals.
All single crystals of the host complexes (compounds I, II, IX and XV) were air stable.

2.1.4 Crystal growth of the clathrates.

Single crystals of all clathrates were prepared by initially making saturated solutions of the host powder complexes in the prospective guest liquids. This was to ensure that the guest concentration was always far in excess of that of the host to maintain the extent of clathration at a maximum.
All the clathrates listed in table 2.1

could be crystallized by either the slow evaporation or liquid diffusion methods; however generally the latter method yielded better quality crystals.
Single crystals of the xylene clathrates (compounds IV, V, VI, X, XI and XII), the CS_2 clathrate (compound VII) and one of the CCl_4 clathrates (compound III) were all dark blue octahedra (illustrated in fig 2.1).
Blue plate-shaped crystals were obtained for the clathrates of $CHCl_3$ (compound XIII) and CCl_4 (compound VIII).

Both CCl_4 clathrates were initially obtained from a single solution by the liquid diffusion method. Octahedra (compound III) formed at the interface while the plate-shaped crystals (compound VIII) grew in the lower half (more concentrated in CCl_4) of the solution.

Green cubic crystals of compound XIV were obtained by both liquid diffusion and evaporation methods whenever the solution used was $[Ni(NCS)_2(4\text{-Etpy})_4]$ host powder dissolved in ethylbromide.

The single crystals of all the clathrates, on exposure to ambient conditions, initially crack and become non-transparent because of surface decomposition (loss of surface guest) and eventually crumble to the host powder, while still retaining the overall shape of the original clathrate crystal , as the internal guest molecules escape.

Fig.2.1 illustrates:

a) A needle-shaped α-phase crystal of compound IX.

b) A typical β-phase octahedral clathrate crystal (compound X) with decomposed crystals from the same solution alongside .

c) A β-phase clathrate crystal (compound X) decomposing by cracking.

Fig.2.1

a) An α-phase crystal of compound IX.

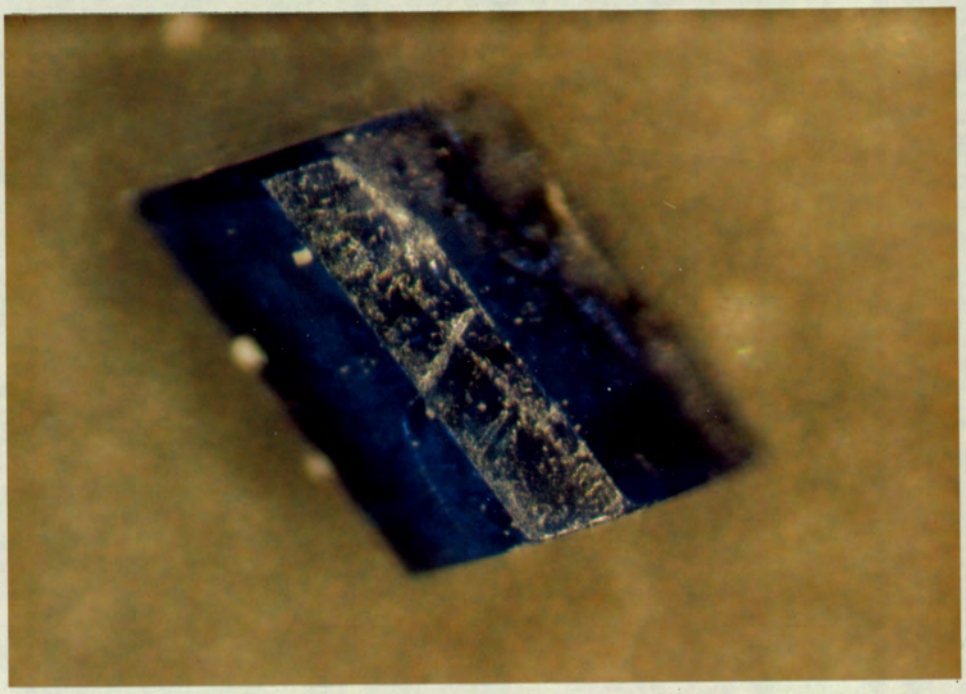

b) A β-phase crystal of compound X with decomposed crystals from the same solution alongside.

Fig.2.1

c) A β-phase clathrate crystal of compound X decomposing by cracking.

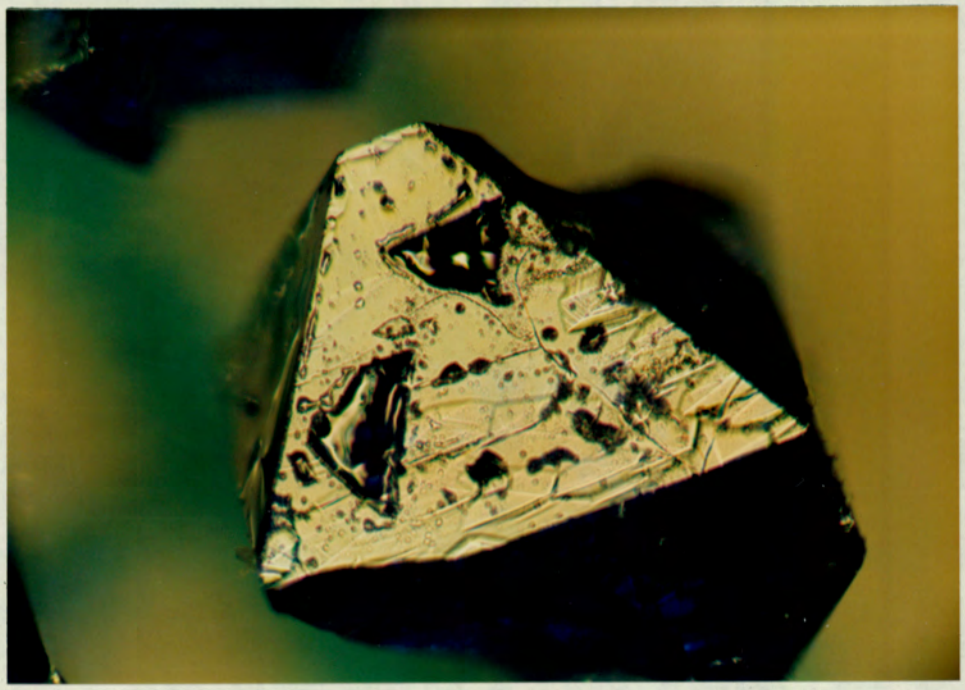

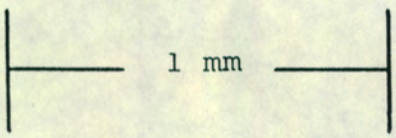

The rate of the decomposition process, which was followed by observing the crystals' behaviour under a microscope, varied for the different clathrates. The clathrates containing $2CS_2$, $2CCl_4$, and $2CHCl_3$ as the guest molecules decomposed more rapidly than the xylene clathrates , and of the latter crystals the p-xylene clathrates had the longest visible stability , hence suggesting a more strongly held guest in the p-xylene clathrate.

2.2 PHYSICAL METHODS

2.2.1 Microanalysis

Microanalysis was used to ascertain the carbon, hydrogen and nitrogen content of each compound.

All determinations were performed on an Hereaus Universal Combustion Analyser, Model CHN-MICRO after Monar[2.4].

Before crystallization, microanalysis was carried out on each host powder to check its purity.

There is good agreement between calculated values and the microanalysis results obtained for the C, H and N composition of each host powder, viz:

Host powder	Measured			Calculated		
	%C	%H	%N	%C	%H	%N
$[Ni(NCS)_2(4\text{-Etpy})_4]$	59.2	5.6	13.7	59.7	6.Ø	13.9
$[Ni(NCS)_2(4\text{-Vipy})_4]$	6Ø.5	4.7	13.8	6Ø.5	4.7	14.1
$[Ni(NCS)_2(3,5\text{-diMepy})_4]$	59.7	5.9	14.Ø	59.7	6.Ø	13.9

Similarly, microanalysis was used prior to any structural investigations carried out on the single crystals. Care was taken not to damage the clathrate crystals in order to keep crystal deterioration to a minimum.

2.2.2 Mass Spectrometry

Mass spectrometry was used as a qualitative identification of the presence and type of guest species in the clathrate crystals.

All spectra were recorded on a V. G. Micromass 16F Spectrometer operating under the following conditions:

Electron beam energy	70eV
Accelerating voltage	4kV
Source Temperature	170 - 200°C

The shapes of the total ion current spectra of the non-clathrated α-phase hosts, compounds I, II and IX, are the same (illustrated in fig. 2.2a). Their fragmentation patterns are similar (listed in table 2.3) and remain the same in all spectra of their different clathrate crystals. In each case the molecular ligand radical peak (m/e = 107 for 4-Etpy and m/e = 105 for 4-Vipy) is one of the most intense peaks (see table 2.3) and was therefore used to monitor host breakdown in the ion current spectra of its clathrates. In general the total ion current spectrum of a clathrate of any of these Werner complexes revealed two distinct peaks (fig. 2.2b). From fragmentation patterns it appeared that during scans of the first peak breakdown of only the guest molecules occurred, while at higher scan numbers the fragments observed related to only the host structure. Hence, for example, scans 1 to 13 in the total ion current spectrum of compound XIII constituted fragments with m/e

Fig.2.2 Total ion current spectrum of:

a) Compound I or II

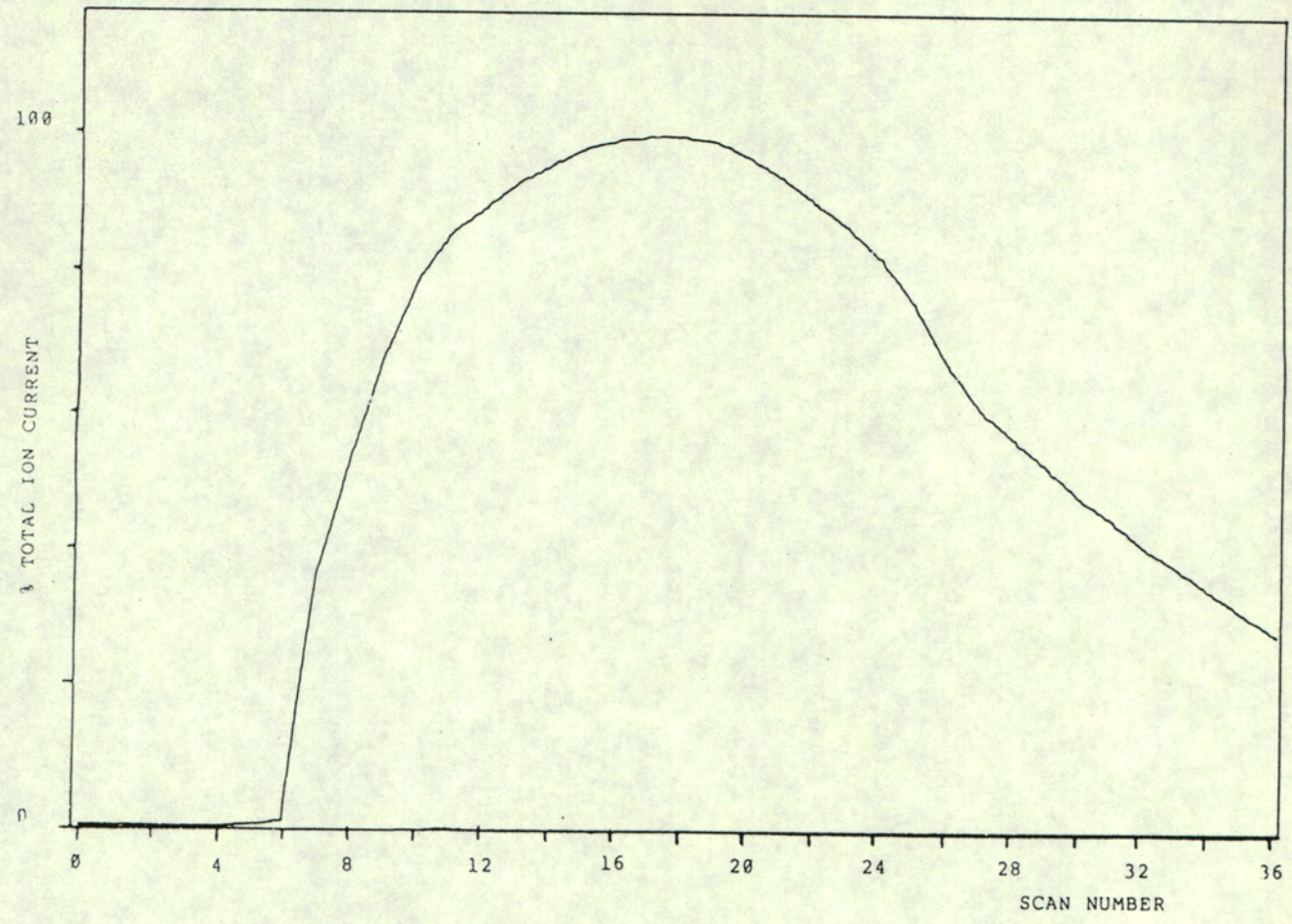

b) Compound XIII

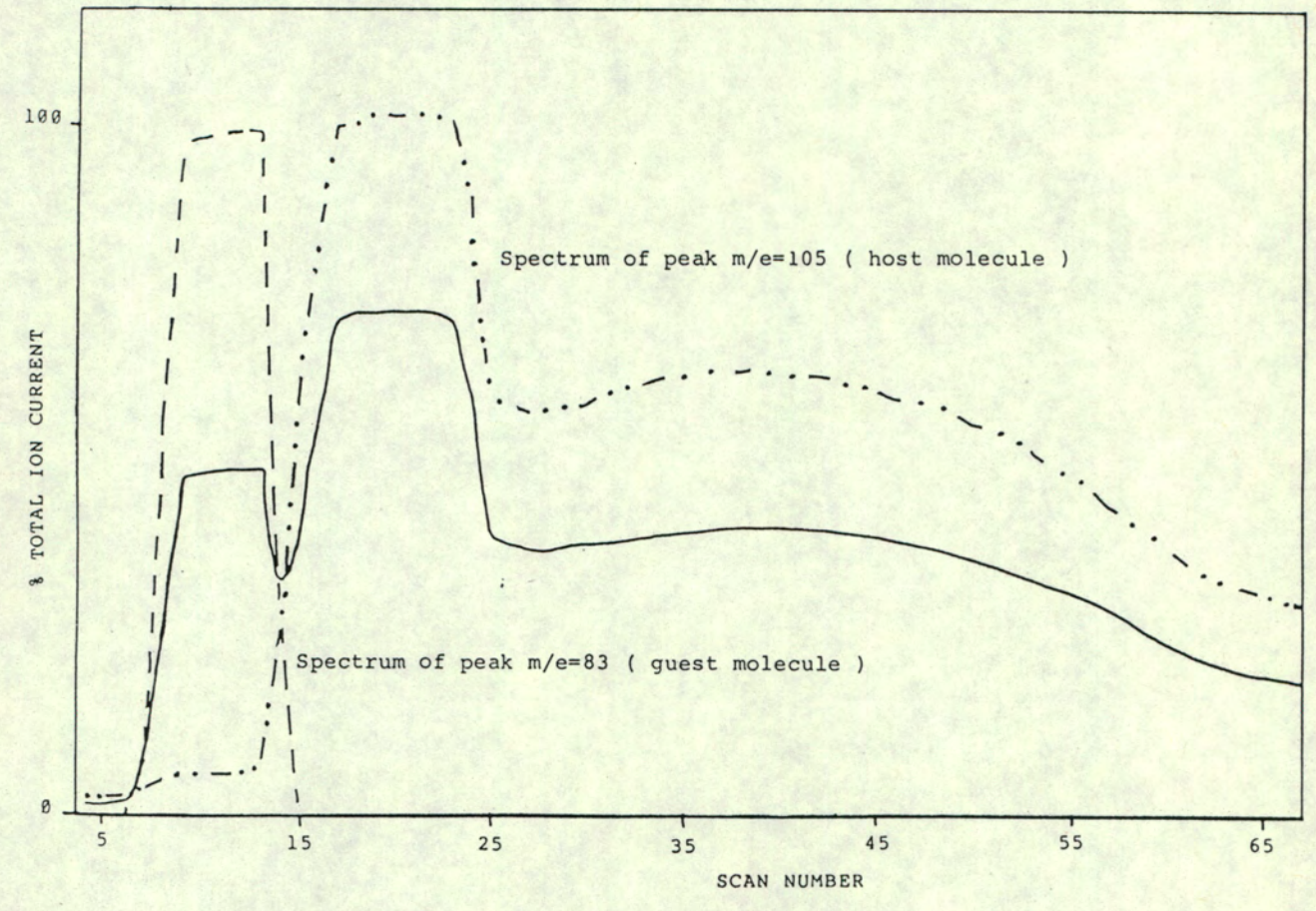

TABLE 2.3 Mass Spectra Fragmentation Patterns of:

a) $[Ni(NCS)_2(4\text{-Etpy})_4]$ host complex

m/e Fragment	% Abundance	Possible Inference
107	100	$C_7H_9N^+$
106	100	$C_7H_8N^+$
92	69	$C_6H_6N^+$
79	34	$C_5H_5N^+$
65	38	$C_5H_5^+/C_4H_3N^+$
51	25	$C_4H_3^+$
39	24	$C_3H_3^+$

b) $[Ni(NCS)_2(4\text{-Vipy})_4]$ host complex

105	100	$C_7H_7N^+$
104	37	$C_7H_6N^+$
78	32	$C_5H_4N^+$
77	13	$C_5H_3N^+$
52	16	$C_4H_4^+$
51	20	$C_4H_3^+$
50	11	$C_4H_2^+$

values of 47 and 83 corresponding to the breakdown of the chloroform guest molecules only. In all subsequent scans fragments corresponding to host breakdown were observed. This is clearly illustrated in fig. 2.2b by superimposition of spectra of both a host fragment (eg: m/e = 105 from 4-Vipy breakdown) and a guest fragment (eg: m/e = 83 which is the CCl_3^+ fragment from CCl_4 breakdown) on the total ion current.

In some of these clathrates simultaneous breakdown of both host and guest molecules occurred during scans of the first peak followed in later scans by host breakdown only.

This illustrates the fact that the guest molecules, being held in the lattice by relatively weak non-bonded interactions, are vaporised before the bonded host ligands.

2.2.3 UV/Visible Spectrophotometry

UV spectra of various solutions of $[Ni(NCS)_2(4\text{-Vipy})_4]$ and $[Ni(NCS)_2(4\text{-Etpy})_4]$ (some of the solvents listed in table 2.2 were used) were obtained to determine whether, in solution, electronic interactions between host and guest molecules are detectable.

All spectra were recorded in the range 190-750nm on a Unicam SP-700 spectrophotometer using 1cm quartz cells.

2.2.4 Density

The host : guest stoichiometry in the clathrates was determined by careful measurement of the single crystal densities.

Because these clathrates decompose, the density column technique was chosen as being the most rapid method of measurement[2.5]. Two linear density columns were prepared in the ranges 1.ØØ to 1.3Ø g/cm^3 and 1.3Ø to 1.63 g/cm^3 using water and KI solution as the two liquids. The column was calibrated with oil droplets of predetermined densities, and a single measurement could be carried out in approximately five seconds.

The observed densities and corresponding host : guest ratios are listed in the tables of crystal data.

The crystal densities of the non-clathrated Werner complexes were also obtained by using the already established columns although the rapid measurement feature was not required.

2.2.5 X-Ray Analysis

In this work both powder and single-crystal X-ray diffraction were utilised.

Single-crystal diffractometry was employed to elucidate the structures of both the α-phase complexes and their clathrates.

Powder diffractograms were utilised primarily to study the kinetics of clathration, which is otherwise difficult to follow, by monitoring changes in the host lattice on desorption of guest molecules.

They also provide a fast method of distinguishing the unclathrated crystalline form of the host complex from its clathrated forms.

All details pertaining to the equipment used in the X-ray analyses are listed in table 2.4.

TABLE 2.4 Equipment used in X-ray analyses

X-ray single crystal.....a) photography b) diffractometry

	a)	b)	
Radiation	CuK_α (λ = 1.5418 Å)	MoK_α (λ = Ø.71Ø7 Å)	
Camera type	Stoe	CAD4 (Enraf-Nonius)	Philips PW11ØØ
Camera radius	28.65mm	-	-
X-ray generator	Philips (PW112Ø, PW114Ø)	Philips (PW173Ø)	Philips (PW114Ø)
Operating conditions	4ØkV, 2ØmA	5ØkV, 2ØmA	
Operating temperature	room temperature (2Ø-3Ø°C)	2Ø°C	
X-ray film	3M medical film	-	-
Location	U.C.T. Cape Town	U.C.T. Cape Town	N.P.R.L. C.S.I.R. Pretoria

X-ray powder diffractometry

Radiation	CuK_α (λ = 1.5418 Å)
X-ray camera and generator	Philips (PW1Ø5Ø/8Ø)
Operating conditions	4ØkV, 2ØmA
Counter	1ØØØc/s
time constant	2s
scan speed	2° 2θ/min
operating temperature	21°C
location	U.C.T., Cape Town.

2.2.5.1 Single crystal X-ray diffractometry.

For each structural determination a single crystal of suitable size (usually between Ø.1 and Ø.5 mm in any dimension; exact dimensions are listed in the tables of crystal data), which extinguished uniformly under plane polarized light, was selected. The suitable single crystal of compound XIV however did not extinguish plane polarised light so the external cubic shape represented the internal cubic structure of this compound.

The air stable α-phase crystals (compounds I, II, IX, and XV) were mounted on glass fibres as were compounds XVI and XVII; however the latter two were also coated in a thin layer of transparent glue to prevent deterioration in the atmosphere. All the other unstable clathrate crystals had to be mounted by wedging and sealing them in a Ø.5 mm diameter Lindemann-glass capillary partly pre-filled with mother liquor at its tip portion to ensure the crystal was either bathed in mother liquor or in its saturated vapour (fig.2.3 illustrates a crystal mounted in this way).

In most cases the space group and approximate cell dimensions were obtained from preliminary oscillation and Weissenberg photographs.

Intensity Data Collections

In the structural determinations of all compounds (except compound XV) accurate lattice constants were determined by

Fig. 2.3

An illustration of the way an unstable clathrate crystal was mounted for its data collection.

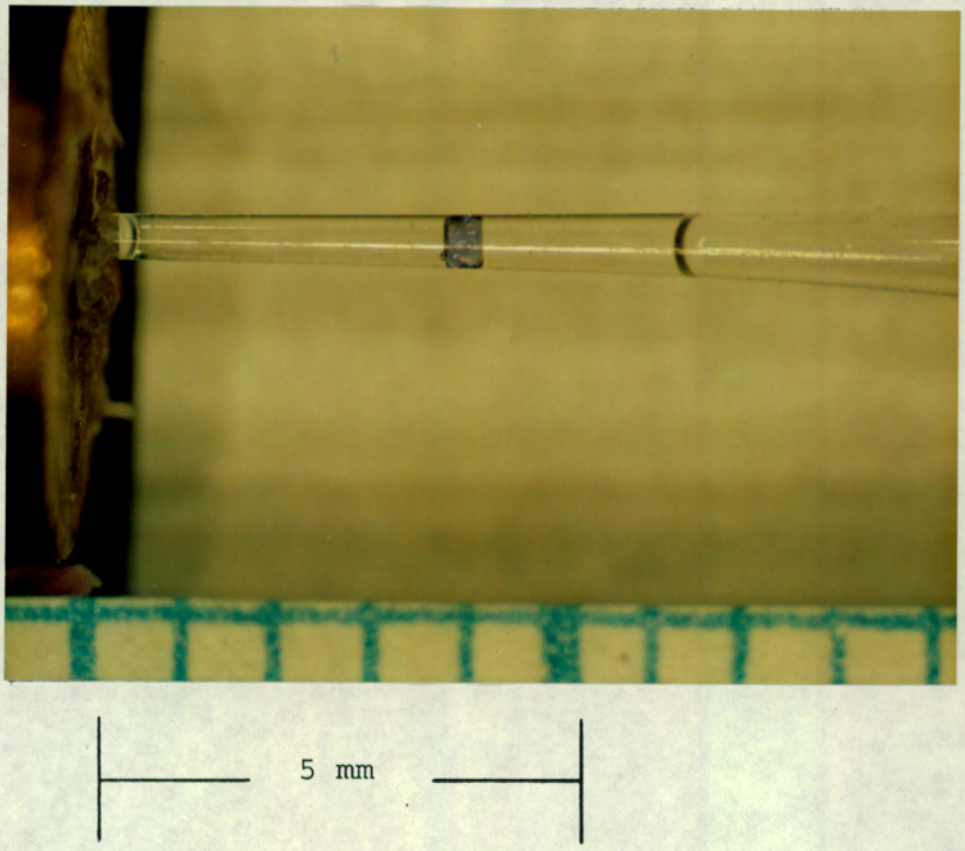

least-squares analysis of 24 reflections measured in the range $16^{\circ} < \theta < 17^{\circ}$ (unfortunately reflections of suitable strength could only be found in the range $12^{\circ} < \theta < 13^{\circ}$ for compound V) automatically located and centred on an Enraf-Nonius CAD4 diffractometer with graphite monochromated MoK_{α} radiation ($\lambda = 0.7107$ Å). Intensity data were collected at 294 K in the $\omega - 2\theta$ scan mode with a final acceptance limit of 20σ at 20°/min in ω and a maximum recording time of 40s.

In each case the intensity variation of three standard reflections was monitored every hour to ascertain both instrumental stability and crystal decomposition and recentring was carried out every 100 measured reflections. All intensities were corrected for Lorentz-polarization and empirical absorption corrections[2.6] were applied to all compounds which remained sufficiently stable during data collection. Compounds V, VII and XII had deteriorated by the end of their data collections; thus it was impossible to carry out absorption corrections. The reflection data of compound XIV were not corrected for absorption as the absorption correction factor, A*[2.7], ranged between 1.35 and 2.07 ($\mu R_{max} = 0.39$, $\mu R_{min} = 0.23$) in the entire θ range scanned. This variation was deemed sufficiently small to be neglected. The reflection data for compound XV were collected at the National Physics Research Laboratory, N.P.R.L., of the Council for Scientific and Industrial Research, C.S.I.R., in Pretoria (see table 2.4) where no facility for absorption corrections was available.

Accurate cell parameters of compound XV were obtained by least-squares from the settings of 25 high-order reflections

measured on a Philips PW1100 computer-controlled four-circle diffractometer, using graphite monochromated MoK_α radiation. Again the intensities of three reference reflections were periodically monitored throughout the data collection and a Lorentz-polarization correction was applied to the data; however no correction was made for absorption.

2.2.5.2 Computation.

All computations were carried out at the University of Cape Town Computer Centre on a Sperry 1100/81 computer.
The programs utilised were:

SHELX-76[2.8]

All structures were solved by the heavy-atom method and subsequent difference Fourier syntheses, with full-matrix least-squares refinement of F magnitudes, using the SHELX-76 program system. The facilities utilised include partial data reduction, rejection of systematic absences, calculation of Patterson and difference Fourier maps, full-matrix least-squares refinement, geometric positioning and constrained refinement of hydrogen atoms, bond length constraints and refinement, analysis of variance, bond length and angle and structure factor listings. The only weighting scheme employed was
$w = (\sigma^2_F)^{-1}$.
When atoms on special positions were treated anisotropically, symmetry restrictions were applied according to Peterse and Palm[2.9].
The agreement between observed (F_o) and calculated (F_c)

structure factors is described in terms of the residual index, R, which is defined as:

$$R = \frac{\Sigma |\Delta F|}{\Sigma |F_o|} = \frac{\Sigma ||Fo| - |Fc||}{\Sigma |F_o|}$$

or as a weighted index:

$$R_w = \frac{\Sigma w^{1/2} |\Delta F|}{\Sigma w^{1/2} |F_o|}$$

Atomic radii used in the program are those of Pauling[2.10]. All complex neutral atom scattering factors for hydrogen were taken from Stewart, Davidson and Simpson[2.11], and for all other atoms from Cromer and Mann[2.12], with dispersion corrections from Cromer and Liberman[2.13].

PARST[2.14]:

All molecular geometry calculations were carried out using PARST - in particular calculations of torsion angles[2.15], weighted least-squares planes (e.s.d.s after Stanford and Waser[2.16]) and intermolecular contacts.

PLUTO and PLUTOX[2.17]:

Individual molecules were drawn using PLUTOX.

PLUTO was used to draw the molecules in their crystalline arrangements to study molecular packing.

Hydrogen atoms were only included to illustrate hydrogen bonding.

XANADU[2.18]:

This program was used to calculate the positions of the terminal vinyl hydrogen atoms for subsequent structure refinement.

It was also used to calculate the coordinates of the ideal m-xylene molecule whose spherical molecular scattering factor was subsequently calculated and used as a disorder model.

ORTEP[2.19]:

This was used to plot the thermal ellipsoids of a $[Ni(NCS)_2(3,5\text{-diMepy})_4]$ molecule in order to obtain a visual comparison of the thermal ellipsoids of the NCS^- groups and the other non-hydrogen atoms; in this way the extent of anisotropy in the NCS^- ligands is displayed.

EENY[2.20]:

Potential energy calculations of both intra- and intermolecular non-bonded interactions occurring in some of the structures have been carried out using the technique of atom pair potentials. With the program EENY the van der Waals energy was evaluated using atom-atom potentials of the form:

$$U(r) = a \exp(-br)/r^d - c/r^6$$

where r is the distance between any pair of atoms and coefficients a, b, c, and d are those given by Giglio[2.21], Quagliata, Scarcelli and Pavel[2.22] such that U(r) is evaluated in kilocalories when r is in Angstroms.

OPEC[2.23]:

Gavezzotti's program OPEC was used to map precisely the sizes and shapes of the guest cavities.

The program is based on standard molecular geometries and atomic radii established by Bondi[2.24] and provides an

accurate method of computing molecular volume. This molecular property introduces the concept of volume analysis in structured media in simple terms of empty and filled space.

MULTAN[2.25]:

The MULTAN 78 program NORMAL was used to calculate the spherically averaged molecular scattering factor for a m-xylene molecule. This was used as a model to map the disorder of the guest in the structure solution of compound XI, $Ni(NCS)_2(4\text{-Vipy})_4$ .m-xylene.

2.2.6 Infra-Red Spectrophotometry

I.R. spectra of the complexes and clathrates as Nujol mulls were obtained on a Perkin Elmer 983 I R Spectrophotometer using CsI sample plates.

2.2.7 Thermal Analysis[2.26]

The physicochemical nature of a Werner clathrate can be better understood by a study of the thermochemistry of its decomposition reaction.

Single crystals of all compounds were first gently dried with tissue paper, care being taken not to crush the crystals, before any thermogravimetric work was carried out.

Thermal analyses were carried out in order to:

a) Confirm the stoichiometry of the clathrates.

b) Obtain the temperature at which guest molecules are released from a clathrate and study the thermochemistry of this `guest-release' reaction.

c) Study the breakdown of the host complex.

All thermograms were carried out on a Stanton-Redcroft Thermal Analyzer (model STA 78Ø), operating at a heating rate of 2Ø^{o}C/min (starting at 4Ø^{o}C and going up to 4ØØ^{o}C). During each run nitrogen was passed through the cell at a rate of 87ml/min.

The reference material used in each case was inert alumina (Al_2O_3).

In the sample holder assembly (illustrated in fig.2.4a) each platinum crucible sits directly on top of its thermocouple; thus only the furnace temperature can be measured directly. The lag between this and the sample temperature was obtained by running a series of standard samples and plotting the furnace temperature required for melting ($T_{furnace}$) versus the known melting point (T_{melt}) as illustrated in fig.2.4b.

Hence the sample temperature ($T_s = T_{melt}$) was calibrated against the furnace temperature. All temperatures quoted are sample temperatures that have been obtained from this calibration curve.

Fig.2.4a) Sample holder assembly of the Stanton Redcroft STA-780 simultaneous TG/DTA system[2.26].

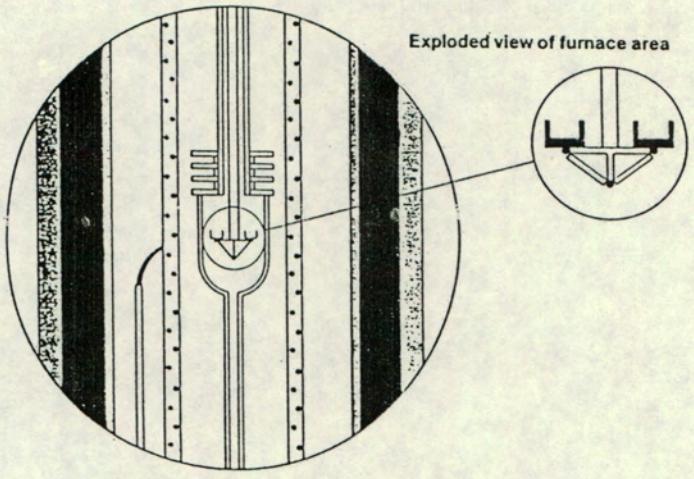

b) Calibration curve of furnace temperature ($T_{furnace}/^{o}C$) versus sample temperature ($T_{melt}/^{o}C$).

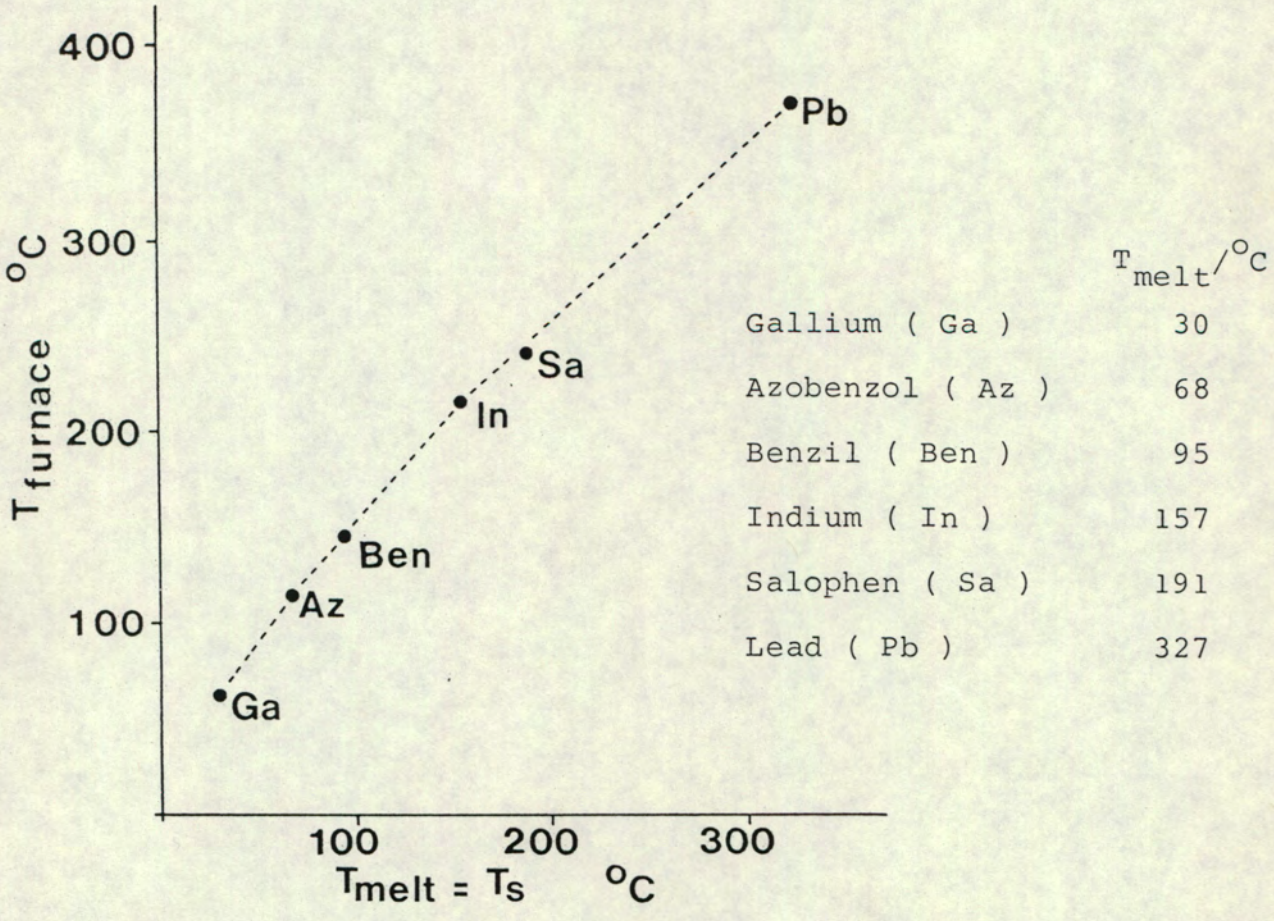

	$T_{melt}/^{o}C$
Gallium (Ga)	30
Azobenzol (Az)	68
Benzil (Ben)	95
Indium (In)	157
Salophen (Sa)	191
Lead (Pb)	327

2 REFERENCES

2.1 W. D. Schaeffer, W. S. Dorsey, D. A. Skinner, J. Christian; **J. Am. Chem. Soc., 79,** 587Ø (1957).

2.2 L. R. Nassimbeni, M. L. Niven, M. W. Taylor; unpublished results.

2.3 C. Orvig; **J. Chem. Ed., 62,** 82 (1985).

2.4 I. Monar; **Mikrochim. Acta** (Wien), 784 (1972).

2.5 G. Oster, M. Yamamoto; **Chem. Rev., 63,** 257 (1963).

2.6 A. C. T. North, D. C. Phillips, F. S. Mathews; **Acta Cryst., A24,** 351 (1968).

2.7 `International Tables for X-ray Crystallography', edited by J. S. Kasper, K. Lonsdale; Kynoch Press, Birmingham, vol II (1967).

2.8 G. M. Sheldrick; SHELX-76 program system in ` Computing in Crystallography ', edited by H. Schenk, R. Olthof-Hazekamp, H. van Koningsveld, G. C. Bassi; Delft Univ. Press, 34 (1978).

2.9 W. J. A. M. Peterse, J. H. Palm; **Acta Cryst., 2Ø,** 147 (1966).

2.1Ø L. Pauling; ` The Nature of The Chemical Bond ', Cornell Univ. Press, Ithaca, New York.

2.11 R. F. Stewart, E. R. Davidson, W. T. Simpson; **J. Chem. Phys., 42,** 3175 (1965).

2.12 D. T. Cromer, J. B. Mann; **Acta Cryst., A24,** 321 (1968).

2.13 D. T. Cromer, D. Liberman; **J. Chem. Phys., 53,** 1891 (197Ø).

2.14 M. Nardelli; **Comput. Chem., 7,** 95 (1983).

2.15 W. Klyne, V. Prelog; **Experientia, 16,** 521 (196Ø).

2.16 G. Stanford, J. Waser; **Acta Cryst, A28,** 213 (1972).

2.17 W. D. S. Motherwell; PLUTO and PLUTOX programs for plotting molecular and crystal structures. Cambridge Univ., England, unpublished.

2.18 P. J. Roberts, G. M. Sheldrick; Cambridge Univ., unpublished.

2.19 C. K. Johnson; ORTEP plotting program, Report ORNL-3794, Oak Ridge National Laboratory, Tennessee (1965).

2.2Ø W. D. S. Motherwell; ` EENY Potential Energy Program ' Univ. Chem. Laboratories, Cambridge (1974).

2.21 E. Giglio; **Nature (London), 222,** 339 (1969).

2.22 N. V. Pavel, C. Quagliata, N. Scarcelli; **Z. Kristallogr., 144,** 64 (1976).

2.23 A. Gavezzotti; ` OPEC Organic Packing Energy Calculations Program ', **J. Am. Chem. Soc., 1Ø5,** no 16, 522Ø (1983).

2.24 A. Bondi; **J. Phys. Chem., 68,** 441 (1964).

2.25 P. Main, S. E. Hull, L. Lessinger, G. Germain, J-P. Declercq, M. M. Woolfson; MULTAN 78; A System of Computer Programs for the Automatic Solution of Crystal Structures from X-ray Diffraction Data (Universities of York, England, and Louvain , Belgium) (1978).

2.26 M. E. Brown; ' Getting Started in Thermal Analysis '; Rhodes University, South Africa (1985).

CHAPTER 3

3 Characterization and structure determination of the Host and Host-Guest Complexes of $[NiX_2B_4]$ where X can be NCS^- or Br^- and B 4-Etpy or 4-Vipy.

3.1 Initial Characterization of the compounds

3.1.1 Microanalysis

The compound formulae and their corresponding numbers have been listed in table 2.1.

All experimentally measured and calculated values of the carbon, hydrogen and nitrogen content of each compound are listed in table 3.1.

After exposure to the air all the clathrates decompose to finally give the same microanalysis results as were obtained for the non-clathrated complex.

The comparability between measured and calculated results reflects the visual stability (section 2.1.4) of these clathrates. They can be arranged in order of decreasing visible stability as follows:

most least

stable X,III,IV > XI,XII,V,VI > XIII > VIII > VII stable.

Compound VII, with its volatile CS_2 guest molecules, was the most unstable clathrate to handle and correspondingly has the greatest difference between measured and calculated values of its C, H and N content. Compounds X, III, and IV, visibly the most stable of the clathrates, showed the best agreement between results and calculated values.

TABLE 3.1 Microanalysis results on $[NiX_2B_4]$ complexes and their clathrates.

Compound; Host.nGuest	Measured			Calculated		
	%C	%H	%N	%C	%H	%N
I; $[Ni(NCS)_2(4\text{-Etpy})_4]$	59.7	6.Ø	13.9	59.7	6.Ø	13.9
II; "	59.6	6.1	13.8	59.7	6.Ø	13.9
III; " .1/2CCl_4	53.8	5.4	12.3	53.8	5.3	12.3
IV; " .p-xylene	64.3	6.4	11.9	64.3	6.5	11.8
V; " .m-xylene	64.1	6.6	12.4	64.3	6.5	11.8
VI; " .o-xylene	64.Ø	6.6	12.5	64.3	6.5	11.8
VII; " .2CS_2	47.8	5.4	11.5	5Ø.8	4.8	11.1
VIII; " .2CCl_4	44.6	4.7	9.9	42.2	4.Ø	9.2
IX; $[Ni(NCS)_2(4\text{-Vipy})_4]$	6Ø.8	4.5	14.Ø	6Ø.5	4.7	14.1
X; " .p-xylene	64.9	5.5	12.Ø	65.1	5.5	12.Ø
XI; " .m-xylene	65.1	5.2	11.9	65.1	5.5	12.Ø
XII; " .o-xylene	65.3	5.3	11.9	65.1	5.5	12.Ø
XIII; " .2$CHCl_3$	46.9	3.6	1Ø.3	46.1	3.6	1Ø.1

Compound; Host.nGuest	Measured			Calculated		
	%C	%H	%N	%C	%H	%N
XIV; $[NiBr_2(4\text{-Etpy})_4]$						
$.2H_2O$	52.1	5.7	9.2	5Ø.6	5.7	8.4
$[NiBr_2(4\text{-Etpy})_4]$				52.8	5.7	8.8
XV; $[Ni(NCS)_2(3,5\text{-diMepy})_4]$						
	58.5	6.1	13.6	59.7	6.Ø	13.9

It was noted that of the two CCl_4 clathrates III and VIII, ~~III~~ was more stable thus suggesting better held guest molecules.

When microanalyses were performed on the pale green colloidal precipitates formed when dissolving either the $[Ni(NCS)_2(4\text{-Etpy})_4]$ or $[Ni(NCS)_2(4\text{-Vipy})_4]$ host powder in various solvents (see section 2.1.2) the composition for each host type always corresponded closest to the dipyridine complex respectively viz:

Measured	$[Ni(NCS)_2(4\text{-Etpy})_2]$			$[Ni(NCS)_2(4\text{-Vipy})_2]$		
%C %H %N	5Ø.6	4.9	13.6	49.Ø	3.8	13.4
Calculated						
%C %H %N	49.4	4.7	14.4	49.9	3.7	14.5

The discrepancy between observed and calculated values indicates possible incomplete decomposition and contamination.

3.1.2 Mass Spectroscopy

The total ion current spectra of three different clathrates of $[Ni(NCS)_2(4\text{-Etpy})_4]$ are illustrated in fig. 3.1.
In each case the ion current spectra for the m/e = 1Ø7 fragment from the breakdown pattern of the 4-ethylpyridine host ligands (table 2.3) and a suitable fragment from the breakdown pattern of the guest molecule are superimposed. In

Fig. 3.1

Mass Spectra of three different clathrates of $[Ni(NCS)_2(4\text{-Etpy})_4]$

a) Compound IV

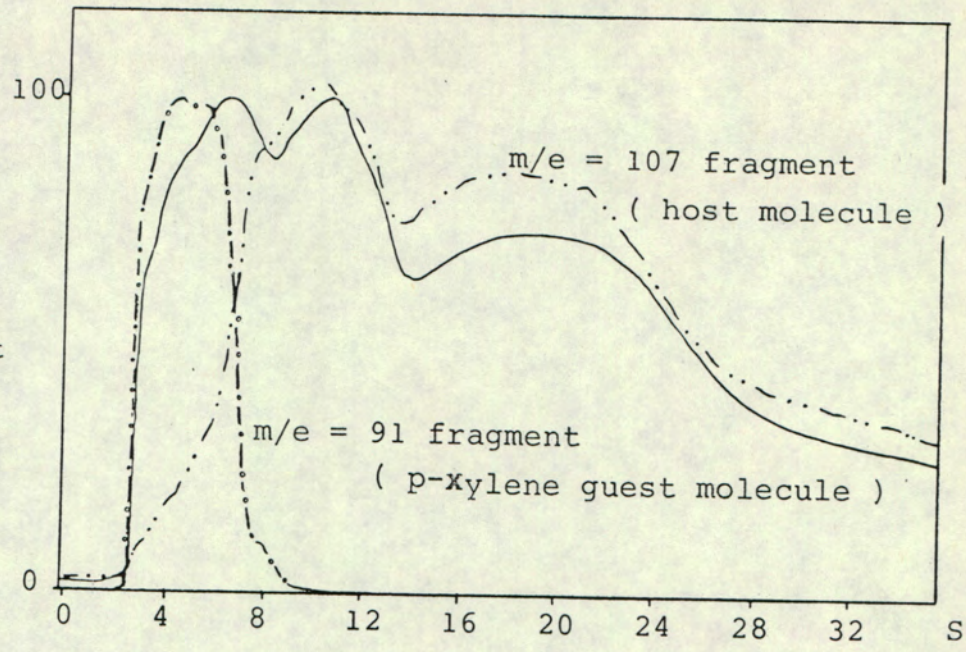

b) Compound III

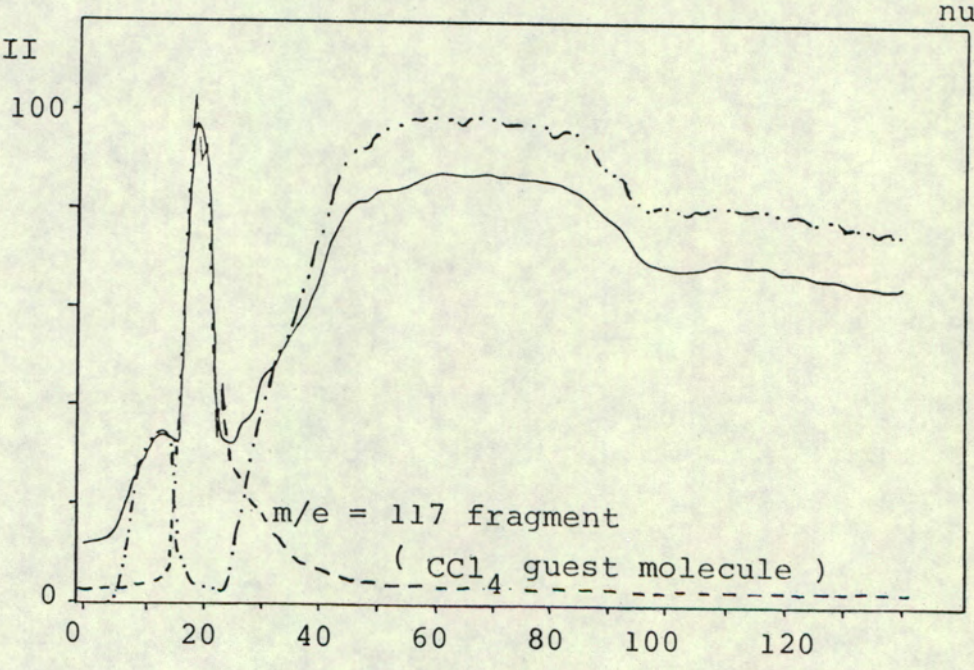

c) Compound VIII

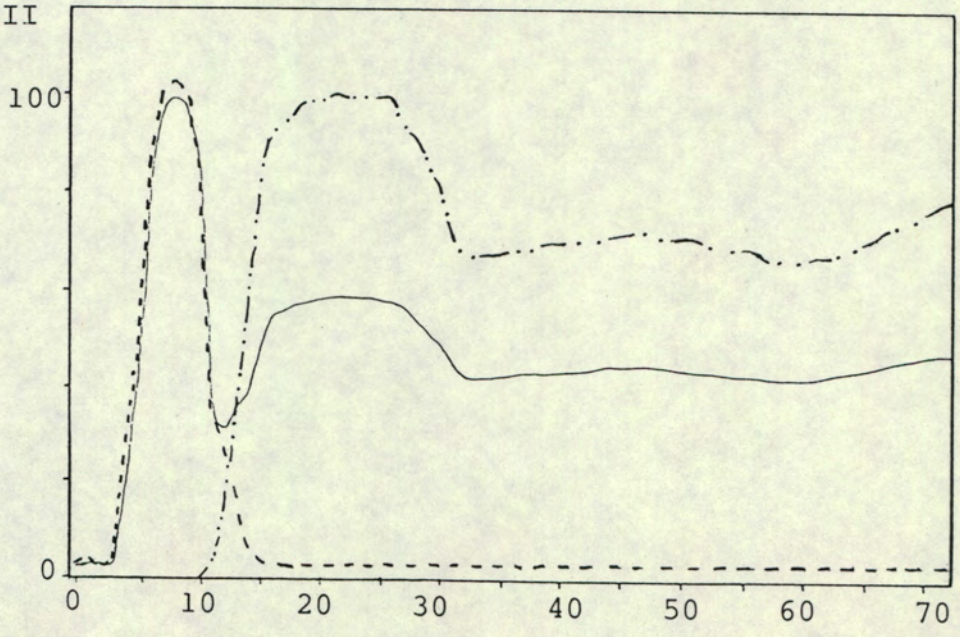

fig. 3.1a) the m/e = 91 fragment is used to monitor the breakdown of p-xylene and in fig. 3.1b) and c) the m/e = 117 fragment illustrates CCl_4 breakdown in compounds III and VIII respectively.

In compound IV simultaneous breakdown of host and guest occurs in the first 2Ø scans followed by host breakdown in subsequent scans. The same pattern is found in compounds V and VI.

By comparison, in compound VIII only the guest decomposes in the first 1Ø scans. This supports its visual behaviour and microanalysis results indicating the more easily removed guest molecules in this clathrate. Compound VII has the same type of spectrum as compound VIII.

The breakdown of compound III reveals some host breakdown in the first 13 scans followed by rapid guest removal in scans 15 to 25 and the bulk host breakdown in subsequent scans. Part of the host has to decompose before the guest can leave again indicating a more strongly held CCl_4 guest molecule than in compound VIII.

The most intense peak in the breakdown pattern of the $[Ni(NCS)_2(4\text{-Vipy})_4]$ complex had m/e = 1Ø5 (see table 2.3) and was used to monitor this fragmentation pattern in all its clathrates. Fig. 2.2b) illustrates the total ion current spectrum of its $CHCl_3$ clathrate, compound XIII, with the spectra of peaks m/e = 83 (monitors $CHCl_3$ breakdown) and m/e = 1Ø5 superimposed to show the early guest escape.

The mass spectra obtained for all the xylene clathrates of this complex were identical to those obtained for the same clathrates of the previous host complex (illustrated in fig. 3.1a)).

The total ion current spectra and corresponding fragmentation patterns of the dipyridine host complex powders , $[Ni(NCS)_2(4\text{-}Etpy)_2]$ and $[Ni(NCS)_2(4\text{-}Vipy)_2]$, obtained in the preliminary solubility studies (section 2.1.2) were identical to those of the corresponding tetrapyridine host complexes, $[Ni(NCS)_2(4\text{-}Etpy)_4]$ and $[Ni(NCS)_2(4\text{-}Vipy)_4]$ (fig.2.2a) and table 2.3). This was as expected since only light fragments, with maximum m/e values of 107 and 105 for the two respective complexes, corresponding to pyridine breakdown were monitored.

3.2 UV-Vis Spectroscopy

All spectra of the solutions of $[Ni(NCS)_2(4\text{-Etpy})_4]$ and $[Ni(NCS)_2(4\text{-Vipy})_4]$ from which single crystals for diffraction were grown, were similar and an example of one such spectrum is illustrated in fig.3.2a.

The strongest peak is at approximately 310nm and may be the result of intermolecular $\pi - \pi$ interactions.

Two other relatively low intensity peaks attributable to ligand field effects of the nickel complexes appear near 360nm and 570nm; they correspond to the $^3A_{2g}(F) \rightarrow {}^3T_{1g}(P)$ and $^3A_{2g}(F) \rightarrow {}^3T_{1g}(F)$ transitions of octahedrally coordinated Ni(II) respectively. The low intensities and positions of the latter two peaks confirm their spin allowed but Laporte forbidden nature, as required by d-d transitions. No additional peaks which may have arisen from electronic intermolecular host-guest interactions were observed in the spectrum of any one of the solutions. Such processes would have given rise to totally allowed transitions and therefore more intense absorptions.

Although these blue solutions do not have the intensity of colour typified by molecular complexes that are said to be involved in `charge-transfer' interactions[3.1], the possibility of a weak force of this nature between the aromatic ligands of the $[Ni(NCS)_2(4\text{-Etpy})_4]$ complex and the halogens of the CCl_4 guest was examined. Spectra of CCl_4 solutions of $[Ni(NCS)_2(4\text{-Etpy})_4]$ at different relative concentrations were recorded to check for any changes in the complex's spectrum (fig.3.2a)) which would occur if the

Fig.3.2

a) Absorption spectrum of $[Ni(NCS)_2(4\text{-Etpy})_4]$ in CCl_4.

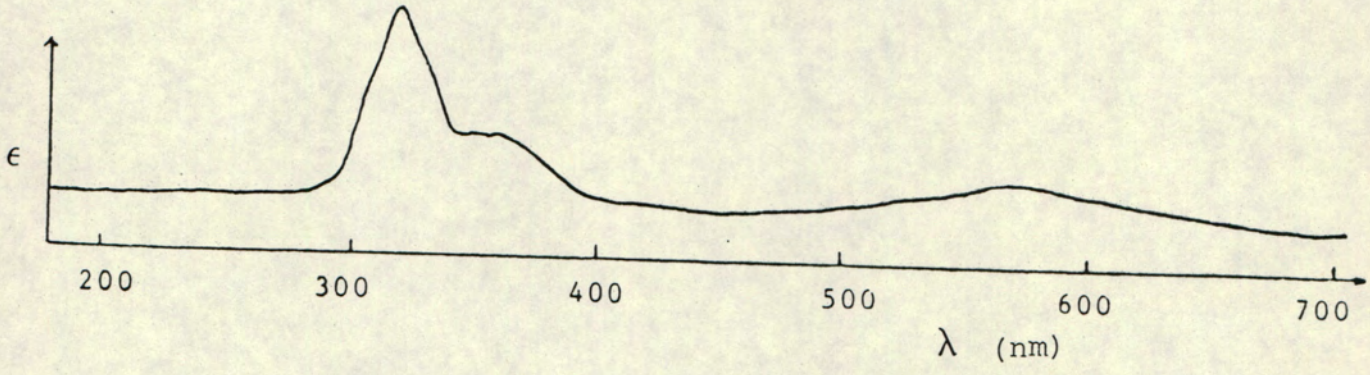

b) Absorption spectra of solutions with different concentrations of $[Ni(NCS)_2(4\text{-Etpy})_4]$ in CCl_4. The slight shift to higher wavelength with increasing $[Ni(NCS)_2(4\text{-Etpy})_4]$ concentration is indicated by the dashed line.

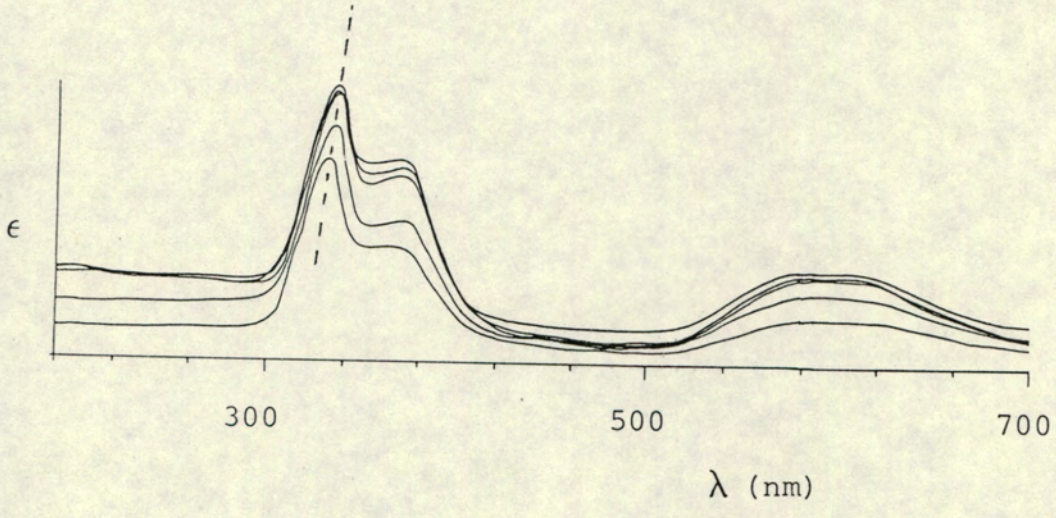

clathrate formed was associated with an electron transfer from one component to the other. The spectra recorded for the various solutions, starting with a saturated $[Ni(NCS)_2(4\text{-}Etpy)_4]$ solution in CCl_4 and halving the Ni(II) complex concentration for each subsequent run, are shown in fig. 3.2b). The slight shift towards higher wavelengths with increasing host concentration in the first peak was not considered sufficient evidence for the existance of a `charge-transfer' interaction between these two molecular species.

3.3 Single Crystal Structures by X-ray analysis

3.3.1 Preliminary X-ray analysis by photography

The single crystal structure determinations of the air stable complexes began with a determination of the geometry of diffraction (from which the size, shape and symmetry of the reciprocal and direct lattices were calculated) by oscillation and Weissenberg photography. Typically a single crystal was mounted on a glass fibre such that the various lattice planes could be brought successively into reflecting positions. This situation was difficult to achieve with unstable clathrate crystals which had to be mounted in Lindemann capillaries (fig. 2.3), and in fact full initial photographic determination of cell constants and space group was only carried out for the two o-xylene clathrates of $[Ni(NCS)_2(4\text{-Etpy})_4]$ and $[Ni(NCS)_2(4\text{-Vipy})_4]$, compounds VI and XII respectively.

3.3.2 X-ray diffraction studies

Crystal data and experimental details of the data collections for:

a) Compounds I to VIII and XIV are listed in tables 3.2 and 3.3

b) Compounds IX to XII are listed in table 3.4

c) Compound XIII and XV are listed in table 3.5.

TABLE 3.2 Crystal Data of $[NiX_2(4\text{-Etpy})_4]$ compounds:

Compound	X	Guest	Molecular Formula	M_r ($gmol^{-1}$)	Host : Guest Ratio	D_m (gcm^{-3})	D_c (gcm^{-3})	μ MoK_α (cm^{-1})	F(000)
I	NCS^-	-	$C_{30}H_{36}N_6NiS_2$	603.50	-	1.23	1.23	7.04	1272
II	NCS^-	-	$C_{30}H_{36}N_6NiS_2$	603.50	-	1.24	1.23	7.02	1272
III	NCS^-	CCl_4	$C_{30}H_{36}N_6NiS_2 \cdot \frac{1}{2}CCl_4$	680.41	2 : 1	1.28	1.28	7.91	2840
IV	NCS^-	p-C_8H_{10}	$C_{30}H_{36}N_6NiS_2 \cdot C_8H_{10}$	709.67	1 : 1	1.27	1.25	6.09	1504
V	NCS^-	m-C_8H_{10}	$C_{30}H_{36}N_6NiS_2 \cdot C_8H_{10}$	709.67	1 : 1	1.22	1.21	5.90	1504
VI	NCS^-	o-C_8H_{10}	$C_{30}H_{36}N_6NiS_2 \cdot C_8H_{10}$	709.67	1 : 1	1.22	1.21	5.93	1504
VII	NCS^-	CS_2	$C_{30}H_{36}N_6NiS_2 \cdot 2CS_2$	755.78	1 : 2	1.38	1.35	8.26	1576
VIII	NCS^-	CCl_4	$C_{30}H_{36}N_6NiS_2 \cdot 2CCl_4$	911.15	1 : 2	1.39	1.39	9.94	932
XIV	Br^-	H_2O	$C_{28}H_{36}Br_2N_4Ni \cdot 2H_2O$	683.18	1 : 2	1.39	1.38	30.49	2052

Compound	Space Group	a (Å)	b (Å)	c (Å)	α (°)	β (°)	γ (°)	V (Å^3)	Z
I	$P\bar{1}$	10.359(5)	16.912(5)	19.398(8)	85.62(3)	83.83(4)	73.83(3)	3241.3	4
II	$P\bar{1}$	10.338(2)	16.113(4)	20.038(2)	91.40(1)	90.83(1)	103.30(2)	3246.6	4
III	$I4_{1/a}$	16.738(4)	16.738(4)	25.174(7)	90	90	90	7052.4	8
IV	$P\bar{1}$	17.425(2)	17.426(3)	17.721(9)	59.49(3)	59.50(3)	61.05(1)	3777.0	4
V	$P\bar{1}$	17.63(3)	17.63(3)	17.749(5)	59.75(8)	59.76(8)	60.5(1)	3898.8	4
VI	$P\bar{1}$	17.61(2)	17.629(3)	17.666(4)	59.92(4)	59.92(7)	60.16(7)	3878.7	4
VII	$P\bar{1}$	17.35(1)	17.36(1)	17.478(6)	59.84(4)	59.79(5)	60.41(6)	3724.0	4
VIII	$P2_{1/c}$	9.356(2)	11.325(6)	20.537(4)	90	92.96(2)	90	2173.0	2
XIV	I432	16.855(4)	16.855(4)	16.855(4)	90	90	90	4788.3	6

TABLE 3.3 Experimental and Refinement Parameters of $[NiX_2(4\text{-Etpy})_4]$ compounds:

Compound	Crystal Dimensions (mm)	DATA COLLECTION: range scanned (°)	Average Transmission (%)	Crystal Stability (%)	Scan Width y[a]	Aperture Width x[b]	Total No. of Reflect^ns	REFINEMENT: Total No. of Obs.[c] Reflect^ns	No. of Variables	R^d	R_w^e	Wght Scheme, w
I	.16x .19x .34	1-25	95.32	1.62	0.53	1.24	11757	3170	371	.072	.072	$(\sigma^2F)^{-1}$
II	.50x .16x .25	1-20	96.37	1.61	0.79	1.13	6275	3898	371	.076	.075	$(\sigma^2F)^{-1}$
III	.44x .44x .38	1-20	95.90	2.54	0.69	1.12	3569	2182	110	.072	.072	$(\sigma^2F)^{-1}$
IV	.22x .25x .34	1-20	98.36	1.42	0.84	1.12	7382	4829	433	.091	.091	unity
V	.56x .44x .38	1-20	-	1.63	0.83	1.11	6651	4771	470	.104	.104	unity
VI	.13x .16x .31	1-20	97.39	2.03	0.60	1.13	6889	4582	470	.105	.105	unity
VII	.25x .31x .38	1-25	-	12.05	0.84	1.12	11877	7415	458	.107	.107	unity
VIII	.25x .63x .38	1-25	95.33	1.49	1.03	1.24	4156	2158	137	.059	.053	$(\sigma^2F)^{-1}$
XIV	.14x .14x .15	1-25	-	1.20	0.74	1.57	453	184	27	.080	.074	$(\sigma^2F)^{-1}$

a) Scan Width, $\Delta\omega$ (°), is given by: (y + 0.35tan θ).

b) Aperture Width (mm), is given by: (x + 1.05tan θ).

c) Observed Reflections are those with $I_{rel} > 2\sigma I_{rel}$.

d) $R = \Sigma \, | \, |F_o| - |F_c| \, | \, / \, \Sigma \, |F_o|$.

e) $R_w = \Sigma \, w^{1/2} \, | \, |F_o| - |F_c| \, | \, / \, \Sigma \, w^{1/2} \, |F_o|$.

TABLE 3.4 Crystal Data and experimental and refinement parameters of:

Crystal Data

Compound	IX	X	XI	XII
Molecular Formula	$C_{30}H_{28}N_6NiS_2$	$C_{38}H_{38}N_6NiS_2$	$C_{38}H_{38}N_6NiS_2$	$C_{38}H_{38}N_6NiS_2$
$M_r/gmol^{-1}$	595.42	701.60	701.60	701.60
Space Group	Pbca	$I4_1/a$	$I4_1/a$	$I4_1/a$
a/Å	11.351(6)	17.039(5)	16.950(3)	16.941(9)
b/Å	16.924(3)	17.039(5)	16.950(3)	16.941(9)
c/Å	32.247(6)	25.508(6)	26.325(6)	26.629(9)
$V/Å^3$	6194.8	7405.7	7563.2	7642.4
Z	8	8	8	8
Host : Guest ratio	-	1 : 1	1 : 1	1 : 1
D_m/gcm^{-3}	1.22	1.26	1.24	1.24
D_c/gcm^{-3}	1.27	1.26	1.23	1.22
$\mu(MoK_\alpha)/cm^{-1}$	65.53	51.86	53.72	53.16
F(000)	2464	2928	2928	2928

Data Collection

Compound	IX	X	XI	XII
Crystal dimensions/mm	.19 x .19 x .47	.50 x .43 x .58	.31 x .31 x .25	.31 x .38 x .44
Scan mode	ω-2θ	ω-2θ	ω-2θ	ω-2θ
Scan width, $\Delta\omega$/°	(0.79+0.35tan θ)	(0.59+0.35tan θ)	(0.54+0.35tan θ)	(0.64+0.35tan θ)
Vertical aperture length/mm	4	4	4	4
Aperture width/mm	(1.66+1.05tan θ)	(1.13+1.05tan θ)	(1.12+1.05tan θ)	(1.11+1.05tan θ)
Final acceptance limit	20σ at 20°min^{-1} in ω	20σ at 20°min^{-1} in ω	20σ at 20 °min^{-1} in ω	20σ at 20 °min^{-1} in ω
Max recording time/s	40	40	40	40
Total number of reflections	6081	3582	3654	8280
Total number of "observed" reflections {with $I_{rel} > 2\sigma I_{rel}$}	3530	2650	2671	3076
Crystal stability/%	2.3	1.6	1.6	1.7

Final refinement

Number of variables	203	104	107	112
R= $\Sigma \lvert\lvert F_o\rvert - \lvert F_c\rvert\rvert / \Sigma \lvert F_o\rvert$	0.071	0.076	0.09	0.110
R_w= $\Sigma w^{1/2} \lvert\lvert F_o\rvert - \lvert F_c\rvert\rvert / \Sigma w^{1/2} \lvert F_o\rvert$	0.062	0.076	0.09	0.092
Weighting scheme w	$(\sigma^2 F)^{-1}$	UNITY	UNITY	$(\sigma^2 F)^{-1}$

TABLE 3.5 Crystal data and experimental and refinement parameters for compounds XIII and XV.

Crystal Data	XIII	XV
Molecular Formula	$C_{32}H_{30}N_6NiS_2Cl_6$	$C_{30}H_{36}N_6NiS_2$
Molecular Weight / $gmol^{-1}$	832.44	603.51
Space Group	$P2_1/n$	$I4_1/acd$
a / Å	10.435(4)	16.187(8)
b / Å	19.787(6)	16.187(8)
c / Å	19.82(1)	25.30(1)
β / °	99.10(4)	
V / $Å^3$	4040.2	6629.1
Z	4	8
Host : Guest ratio	1 : 2	—
D_m / gcm^{-3}	1.38	1.22
D_c / gcm^{-3}	1.37	1.20
μ (M_o - K_α) / cm^{-1}	9.43	6.12
F(000)	1704	2544

Data Collection	XIII	XV
Scan width, $\Delta\omega$ =	$(0.85 + 0.35\tan\theta)^\circ$	Scan width = $0.40^\circ\theta$
Aperture width =	$(1.30 + 1.05\tan\theta)$ mm	Scan speed = $0.016^\circ\theta\ s^{-1}$
Range scanned / °	$1 < \theta < 25$	$3 < \theta < 23$
Stability of Standard Reflections / %	1.87	1.1
Number of Reflections Collected	7563	2623
Number of 'Observed' Reflections with $I_{rel} > 2\sigma I_{rel}$	3120	978

Final Refinement	XIII	XV
Number of Variables	261	103
$R = \Sigma \| \|F_o\| - \|F_c\| \| / \Sigma \|F_o\|$	.073	.101
$R_w = \Sigma w^{1/2} \| \|F_o\| - \|F_c\| \| / \Sigma w^{1/2} \|F_o\|$	.069	.101
Weighting Scheme	$(\sigma^2_F)^{-1}$	unity

An illustration of the smearing of the electron density around Wyckoff position e in compound V.

On the transparencies:

five sections along the [100] direction (the atoms within these sections are depicted as filled circles).

Below the transparencies:

a section perpendicular to those represented on the transparencies with the m-xylene guest molecules chosen for the disorder model.

Wyckoff position e is represented by an empty circle.

In each structure refinement the final model employed anisotropic thermal parameters for all heavy atoms (Ni, S, Br, Cl) and isotropic ones for all other atoms.

Aromatic hydrogen atoms were subjected to constrained refinement, riding at 1.08Å from their parent carbon atoms, with a common isotropic temperature factor. The ethyl hydrogens were also placed in calculated positions at 1.08Å from their parent carbon atoms. The CH_2 hydrogens in each case were geometrically positioned to form an ideal secondary CH_2 group with a common temperature factor and the methyl hydrogens were positioned such that the four atoms form a rigid primary CH_3 group (these hydrogens also had their own common temperature factor). The two terminal hydrogens on each vinyl group were placed in calculated positions, 1.08Å from the parent C atom and with an H-C-H angle of 120°, again with a single isotropic temperature factor.

The criteria fulfilled before each structure was considered solved completely were:

a) A low value for the conventional residual, R.
For partially disordered structures R = .10 is generally accepted, however for most cases it was less than this.

b) A low shift/e.s.d. value for each parameter in the final cycle. Values less than 0.1 were obtained for ordered structures, but for disordered moieties higher values were sometimes obtained.

c) A satisfactory analysis of variance (ie: with minimal variation) calculated after the final refinement of each structure; these are listed in Appendix B.

d) Chemically feasible molecular geometry (ie: acceptable coordination, bond lengths and angles).

e) A maximum peak height in the final difference Fourier synthesis corresponding to less than Ø.8 electron/Å^3.

Structure solutions

All structures, except compound XIV, were solved in centrosymmetric space groups as indicated by values of approximately Ø.9 for mean $|E^2 - 1|$ statistics calculated on the observed reflections.

Attempts made to solve any $P\bar{1}$ clathrate structure in P1 resulted in extensive correlation in the L.S. matrix and a high value of the conventional residual, R, substantiating the centrosymmetric nature of these structures.

No hydrogen atoms were inserted on any guest molecule.

Compound IX: $[Ni(NCS)_2(4\text{-Vipy})_4]$; Pbca; a = 11.351(6)Å, b = 16.924(3)Å, c = 32.247(6)Å; Z = 8.

An orthorhombic space group was revealed by m_x symmetry[3.2] in the oscillation photograph together with two mirrored axes 90° apart in the Weissenberg of a single crystal of compound IX. Approximate cell parameters obtained were a = 11.2Å, b = 15.8Å, c = 31.3Å giving a cell volume of 6195Å^3 and consequently (with the crystal density) Z = 8. From the Weissenberg photographs, the conditions for non-extinction of reflections were determined as:

hkl : no condition

Økl : k = 2n

hØl : l = 2n

hkØ : h = 2n which uniquely defined the space group as Pbca.

With eight molecules per unit cell in space group Pbca, the nickel atoms were found to lie on the general positions denoted by Wyckoff as c. The coordinates of the nickel atom closest to the origin were established as x = .Ø7Ø9, y = .ØØØ2, z = .1337 from the highest Ni x Ni Patterson vector types:

1/2, Ø, 2z + 1/2; 1/2, Ø, -2z + 1/2; 2x + 1/2, 1/2, Ø;

-2x + 1/2 , 1/2, Ø; Ø, 2y + 1/2, 1/2; Ø, -2y + 1/2, 1/2.

The first difference electron density map phased on this nickel atom yielded two peaks corresponding to 4 electrons/Å^3, each peak was approximately 4Å from the nickel (typical Ni to S distance for isothiocyanate ligands bonded through the N) and the peak1-Ni-peak2 angle was approximately 18Ø°. The conventional residual, R, was .45 at this stage. A second difference electron density map phased

on the original Ni and the two newly located sulphurs yielded the positions of 14 other non-hydrogen atoms (R = .13). Five other carbon positions were calculated then all 22 atoms were inserted for a third difference Fourier which yielded all remaining non-hydrogen atoms.

Anisotropic treatment of the heavy atoms coupled with the insertion of hydrogen atoms reduced the R to .Ø65. The final difference electron density map revealed no peak corresponding to more than Ø.5 electron/Å^3 in height, confirming the absence of any guest molecule and subsequent molecular packing diagrams revealed that there are no suitable cavities in which prospective guests may have been housed.

Slight disorder in the vinyl moieties was indicated by the fact that the carbon atoms of these groups had higher temperature factors than those in the pyridine rings and the variation in the C_{vinyl} - C_{vinyl} bond distances (see Appendix A).

Fractional atomic coordinates and thermal parameters of compound IX are listed in table 3.6.

Compounds X, XI and XII: $I4_1/a$; Z = 8;

	a (Å)	c (Å)
X $[Ni(NCS)_2(4\text{-}Vipy)_4].p\text{-}C_8H_{1Ø}$	17.Ø39(5)	25.5Ø8(6)
XI $[Ni(NCS)_2(4\text{-}Vipy)_4].m\text{-}C_8H_{1Ø}$	16.95Ø(3)	26.325(6)
XII $[Ni(NCS)_2(4\text{-}Vipy)_4].o\text{-}C_8H_{1Ø}$	16.941(9)	26.629(9).

For each crystal, symmetry displayed in the oscillation and Weissenberg photographs indicated a tetragonal space group.

The cell parameters estimated from the photographs of a single crystal of compound XII were: a = b = 16.8Å, c = 26.7Å with a cell volume of 7643Å^3 indicating Z = 8.

Before any data were collected the required equivalences for the tetragonal 4/m symmetry of each structure, namely $F(hkl) = F(\bar{h}\bar{k}l) = F(\bar{k}hl) = F(k\bar{h}l) = F(\bar{h}\bar{k}\bar{l}) = F(hk\bar{l}) = F(k\bar{h}\bar{l}) = F(\bar{k}h\bar{l})$, were thoroughly checked.

All three xylene clathrates of $[Ni(NCS)_2(4\text{-Vipy})_4]$, compounds X, XI and XII, crystallise in the space group $I4_1/a$ and their structures are reported with respect to the second origin choice at $\bar{1}^{3.3}$. With 8 molecules per unit cell the nickel atom most likely lies on a special position which could either be an inversion centre (denoted by Wyckoff as c or d) or on a two-fold axis (Wyckoff position e). The Patterson did not yield any peaks at the special positions Ø, Ø, Ø or Ø, Ø, 1/2 which ruled out the inversion centres. Instead vector types: 1/2, 1/2, 1/2; Ø, 1/2, 1/4; Ø, 1/2, 3/4; 1/2, Ø, 1/4; 1/2, Ø, 3/4; 1/2, 1/2, 2z + 1/4; 1/2, 1/2, - 2z + 1/4; Ø, Ø, 2z + 3/4; Ø, Ø, - 2z + 3/4 located in the Patterson led to positioning of the nickel atom at 1/2, 1/4, .55 with a site occupation factor of 1/2. The first difference electron density map calculation yielded the position of the sulphur atom (R = Ø.46). The remaining atoms constituting the asymmetric unit (two pyridine rings and the nitrogen and carbon of the isothiocyanate ligand were subsequently located and refined. The difference Fourier map obtained after the refinement of the host atoms yielded several peaks of high electron density (3 and 2 electrons/Å^3) indicating the presence of a guest molecule. Several of the bond lengths involving the vinyl carbon atoms

are outside the usually quoted limits. Their isotropic temperature factors are consistently higher than those of the pyridine-ring carbons thus indicating some disorder in these moieties.

For compound X the p-xylene guest was located around Wyckoff position d, an inversion centre. The atoms were well ordered and yielded acceptable bond lengths and angles, although their isotropic temperature factors remained consistently higher than those of the aromatic carbon atoms in the host molecule. The non-centrosymmetric xylene guest molecules in both compounds XI and XII were also located around Wyckoff position d. A difference electron density map was calculated and contoured and the centrosymmetric electron density of the guest could only be chemically interpreted by invoking a disorder model. Two different attempts were made at modelling this combination of static and dynamic disorder:

a) Molecular Scattering Factor:

This model was initially employed in an attempt to interpret the m-xylene disorder. It has been successfully used for the location of a two-fold disordered (+)-camphor molecule in the 2 : 1 complex between deoxycholic acid and camphor[3.4]. A "molecular scattering factor" was employed to model the disordered camphor, which improved the model of the rest of the structure and in turn allowed improved resolution of the disordered camphor moieties. In a similar manner the spherically-averaged molecular scattering factor for m-xylene using an ideal model (a regular hexagon with the two idealised methyl groups attached meta to each other and 1.4 Å from their parent C atoms) was employed

for the coordinate input to NORMAL of MULTAN[3.5]. An approximation of the scattering with sin θ / λ was then obtained in the form suitable for SHELX76[3.6],

$$f(x) = a_1 e^{-b x} + a_2 e^{-b x} + a_3 e^{-b x} + c,$$

by the addition of normal distribution functions[3.7]. The result obtained is shown in fig. 3.3. This spherically-averaged group scattering factor was then placed on Wyckoff position d, which was the centroid of the high electron density peaks, and refined isotropically. Residual electron density in the subsequent difference electron density map nowhere exceeded 1 e/Å^3 but standard deviations of the parameters of the host molecules were not reduced. On removal of the group scatterer, the difference map obtained without further refinement yielded four peaks which were not significantly different from those obtained initially.
The lack of success of this model can be atributed primarily to the fact that m-xylene is not spherically shaped and secondly that the the degree of disorder is not very high.

b) Rigid-body Model:

In this model different orientations of a chemical group, each of which represents an energetically favourable orientation within its crystalline environment, are located. Atoms of this group are then inserted to fulfill all these orientations, fixing bond lengths and angles where necessary, and assigning fractional site occupancy factors. The best model for refinement of the two non-centrosymmetric xylene guests in compounds XI and XII was achieved by fitting half of a regular hexagon of carbon atoms, with site occupation factors of unity, and two methyl carbons with

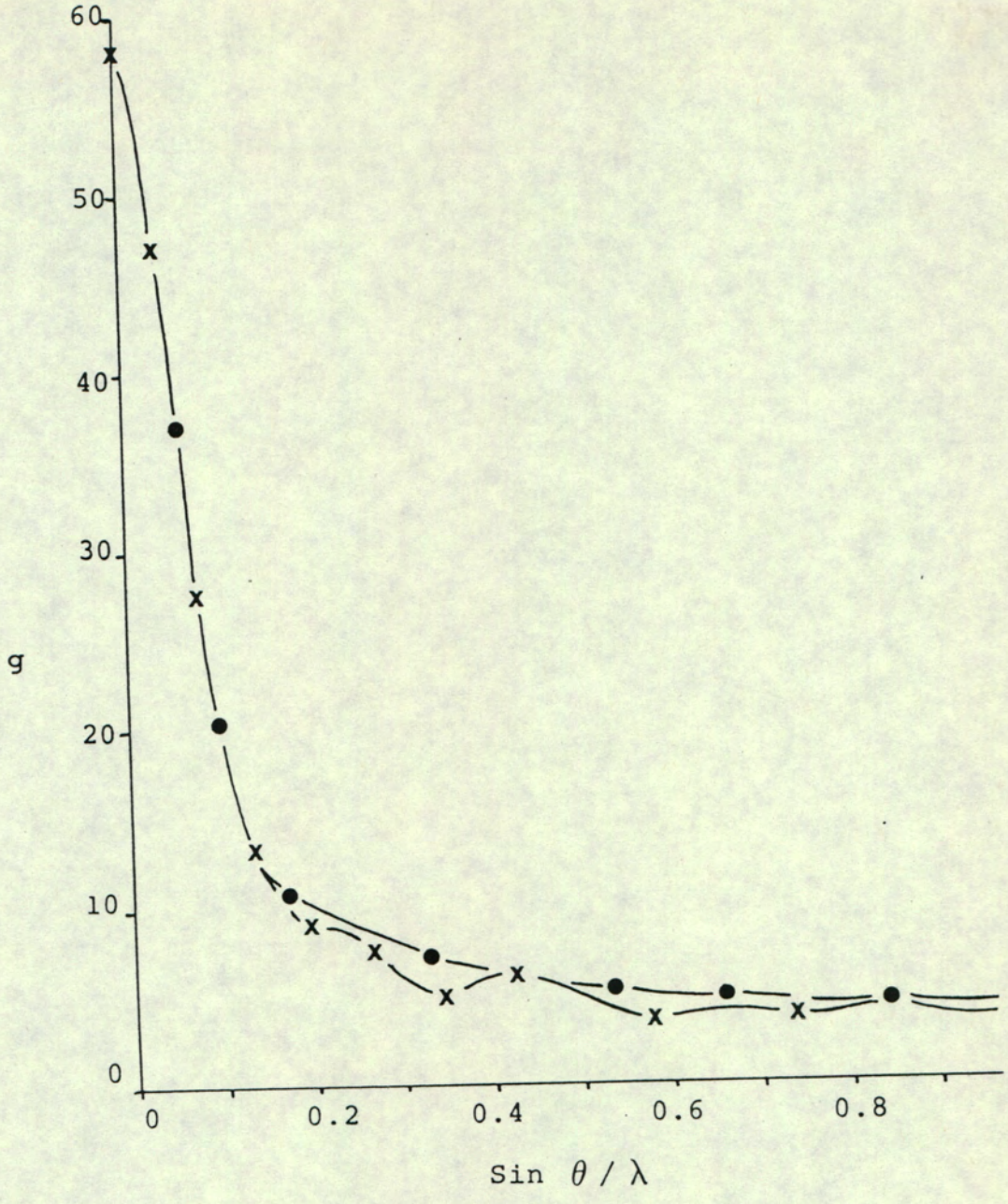

Fig.3.3 Spherically averaged molecular scattering factor for m-xylene as calculated by MULTAN; the expression for the curve fit obtained is

$g = 48.9\exp(-165.3x^2) + 3.8\exp(-6.6x^2) + 2.5\exp(-2.1x^2) + 5.2$

where $x = \sin \theta / \lambda$.

site occupation factors of 1/2.

The isotropic temperature factors of these guest carbons were considerably higher than those of the aromatic carbons of their respective host molecules (see table 3.7). The final difference electron density map calculated after the last full-matrix least squares refinement yielded 4 small peaks (all less than 1 e/Å^3) in the vicinity of the guest molecule. These were accounted for as imperfect modelling of the disordered xylene. There is no evidence, however, of electron density at the tetrahedral site, Wyckoff position b. The X-ray solution of the structure reveals, according to the location of the electron density, that the maximum value for the molar host : guest ratio is 1 : 1 which agrees with the experimentally determined value obtained from the crystal density. All fractional atomic coordinates and thermal parameters of compounds X, XI and XII are reported in table 3.7.

Compounds I and II: $[Ni(NCS)_2(4\text{-Etpy})_4]$; $P\bar{1}$; Z = 4;

	a (Å)	b (Å)	c (Å)	α(°)	β(°)	γ(°)
I	10.359(5)	16.912(5)	19.398(8)	85.62(3)	83.83(4)	73.83(3)
II	10.338(2)	16.113(4)	20.038(2)	91.40(1)	90.83(1)	103.30(2)

The single crystal of compound I is triclinic because of the absence of mirror planes in both oscillation and Weissenberg photographs. Approximate cell dimensions obtained from the photographs were a = 9.6Å, b = 17.2Å, c = 20.0Å, α = 85°, β = 85°, γ = 75°, giving a cell volume of 3171Å^3 and together with the measured crystal density, a